Supporting Information

Stepwise Cyclopropanation on the Polycyclopropanated Polyketide Formation in Jawsamycin Biosynthesis

Tomoshige Hiratsuka, Hideaki Suzuki, Atsushi Minami, and Hideaki Oikawa*

Division of Chemistry, Graduate School of Science, Hokkaido University, Sapporo 060-0810, Japan.

Table of Contents

General.

All reagents commercially supplied were used as received. ^{1}H- and ^{13}C-NMR spectra were recorded on Bruker AMX-500 spectrometer. NMR spectra were recorded in $(CD_3)_2SO$ (99.9 atom % enriched, Kanto). ^{1}H chemical shifts were reported in δ value based on internal $(CD_3)_2SO$ (2.50 ppm) as a reference. ^{13}C chemical shifts were reported in δ value based on dimethyl sulfoxide (39.5 ppm) as a reference. Data are reported as follows: chemical shift, multiplicity (s = singlet, d = doublet, t = triplet, q = quartet, m = multiplet, br = broad), coupling constant (Hz), and integration. Mass spectra were obtained with a JEOL JMS-T100LP (ESI mode). Tandem MS analysis was conducted with a LTQ-Orbitrap XL (ThermoScientific).

Feeding experiments of ^{13}C-labeled methionine.

Seed cultures (3.0 mL) of *S. lividans* TK23 harboring pJawA or pJawB[1] were inoculated to 20 mL of Soytone medium {50 g of D-glucose, 20 g of Soytone, 0.3 g of KH_2PO_4, 0.4 g of K_2HPO_4 and 0.2 g of $MgSO_4$•$7H_2O$ per liter of water (pH 7.0)} containing thiostrepton (10 μg/mL) in 100 mL baffled shake flask and grown at 30°C for 2 days with agitation. The culture broth (0.3 mL) was further inoculated to 5.7 mL of Soytone broth containing thiostrepton (10 μg/ml) in 100 mL baffled shake flask. To this culture was added L-[Me-$^{13}C_1$]methionine (final concentration: 1 mg/mL). Cultivation was continued for an additional 3 days at 30°C. The culture broth was extracted with ethyl acetate and the organic layers were evaporated to dryness under reduced pressure. The crude mixture was dissolved in 300 μL of acetonitrile and the sample solution (10 μL) was directly analysed by LC-MS/MS with InertSustain C18 (1.0 mm x 10 mm, GL science) using a linear gradient from 20% to 38% Solution B for 0–5 min, 38% to 45% for 5–30 min, 45% to 60% for 30–35 min, 60% to 100% for 35–36 min, 100% Solution B additional 9 min. Solution A: 98% of water and 2% of acetonitrile containing 0.1% formic acid, Solution B: 10% of water and 90% acetonitrile containing 0.1% formic acid.

Isolation of jawsamycin analogs.

S. lividans TK23 harboring pJawA or pJawB was grown on Soytone medium (100 mL) containing thiostrepton (20 μg/mL) in baffled shake flask (500 mL). Fermentation was carried out for 1 week at 30°C with agitation. The culture broth (2.4 L) was extracted with ethyl acetate. The organic layers were evaporated to dryness under reduced pressure. The resultant was dissolved in a small volume of DMSO and purified by preparative HPLC. The crude extracts were separated by HPLC with Wakopack Navi C18-5 (10 mm x 250 mm, Wako) [column temperature, 30°C; flow rate, 2.5 mL/min] using a linear gradient from 70% to 74% acetonitrile for 0–14 min, 74% to 95% for 14–15 min, 95% acetonitrile additional 1 min, 95% to 70% for 16–16.5 min, and 70% acetonitrile for an additional 8.5 min. The crude fraction was further separated by the following HPLC conditions to give the following analogs;

3 (C_{16}-CP_5): The crude fraction containing **3** was purified by HPLC with Wakopack Navi C18-5 (10 mm x 250 mm, Wako) [column temperature, 30°C; flow rate, 2.5 mL/min] using a linear gradient from 55% to 55% acetonitrile for 0–17 min, 55% to 90% for 17–18 min, 95% to 55% for 18–18.5 min, and 55% acetonitrile for an additional 8.5 min to yield **3** (1.8 mg).
$[\alpha]_D^{20}$ -98.1 (c 0.094 $(CH_3)_2SO$). ESI-HR-MS (positive) calculated for $C_{30}H_{40}N_3O_6$ $[M+H]^+$ 538.2912,

found *m/z* 538.2936. NMR data of **3** are summarized in Table S3.

4 (C_{16}-CP_4): The crude fraction containing **4** was purified by HPLC with Wakopack Navi C18-5 (10 mm x 250 mm, Wako) [column temperature, 30°C; flow rate, 2.5 mL/min] using a linear gradient from 65% to 65% acetonitrile for 0–14 min, 65% to 95% for 14–15 min, 95% acetonitrile additional 1 min, 95% to 65% for 16–16.5 min, and 65% acetonitrile for an additional 8.5 min to yield **4** (2.6 mg).
$[\alpha]_D^{20}$ -211.3 (c 0.46 $(CH_3)_2SO$). ESI-HR-MS (positive) calculated for $C_{29}H_{38}N_3O_6$ $[M+H]^+$ 524.2755, found *m/z* 524.2727. NMR data of **4** are summarized in Table S3.

2a (C_{18}-CP_4): The crude fraction containing **2a** was purified by HPLC with Wakopack Navi C18-5 (10 mm x 250 mm, Wako) [column temperature, 30°C; flow rate, 2.5 mL/min] using a linear gradient from 72% to 72% acetonitrile for 0–14 min, 72% to 95% for 14–15 min, 95% acetonitrile additional 1 min, 95% to 72% for 16–16.5 min, and 72% acetonitrile for an additional 8.5 min to yield **2a** (1.0 mg).
$[\alpha]_D^{20}$ -60.4 (c 0.087 $(CH_3)_2SO$). ESI-HR-MS (positive) calculated for $C_{31}H_{40}N_3O_6$ $[M+H]^+$ 550.2912, found *m/z* 550.2865. NMR data of **2a** are summarized in Table S3.

3a (C_{16}-CP_4): The partially purified fraction containing **3a** and **4** was further purified by HPLC with Wakopack Navi C18-5 (4.6 mm x 250 mm, Wako) [column temperature, 30°C; flow rate, 1.0 mL/min] using an isocratic condition (48% acetonitrile) to yield **3a** (0.3 mg).
$[\alpha]_D^{20}$ -23.4 (c 0.033 $(CH_3)_2SO$). ESI-HR-MS (positive) calculated for $C_{29}H_{38}N_3O_6$ $[M+H]^+$ 524.2755, found *m/z* 524.2752. NMR data of **3a** are summarized in Table S3.

4a (C_{16}-CP_3): The crude fraction containing **4a** was purified by HPLC with Wakopack Navi C18-5 (10 mm x 250 mm, Wako) [column temperature, 30°C; flow rate, 2.5 mL/min] using a linear gradient from 60% to 60% acetonitrile for 0–14 min, 60% to 95% for 14–15 min, 95% acetonitrile additional 1 min, 95% to 60% for 16–16.5 min, and 60% acetonitrile for an additional 8.5 min to yield **4a** (1.6 mg) as a mixture of isomers (**4a**/isomer = 5/1 ratio).
$[\alpha]_D^{20}$ -39.7 (c 0.10 $(CH_3)_2SO$). ESI-HR-MS (positive) calculated for $C_{28}H_{36}N_3O_6$ $[M+H]^+$ 510.2599, found *m/z* 510.2590. NMR data of **4a** are summarized in Table S3.

References

1. T. Hiratsuka, H. Suzuki, R. Kariya, T. Seo, A. Minami, H. Oikawa, *Angew. Chem. Int. Ed.* **2014**, *53*, 5423-5426.

Figure S1. MS spectra of crude metabolites obtained from (A) dehydrojawsamycin (**2**) producing transformant and (B) jawsamycin (**1**) producing transformant. (C) Isolated dehydrojawsamycin analogs corresponding to the observed molecular ion peaks.

(A)

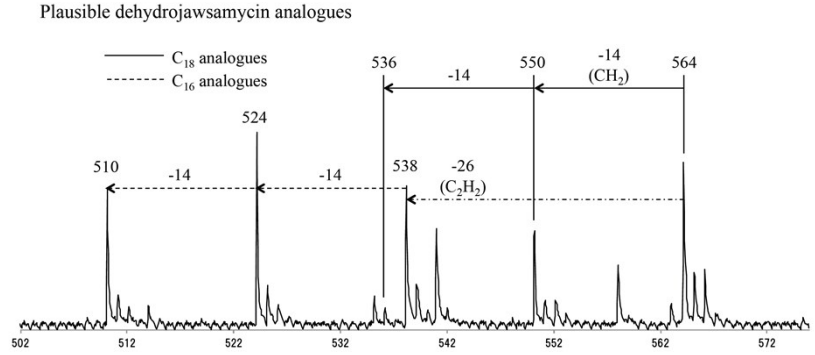

(B)

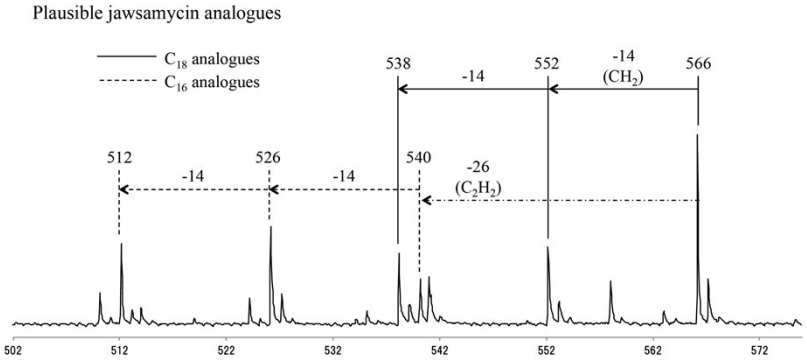

(C)

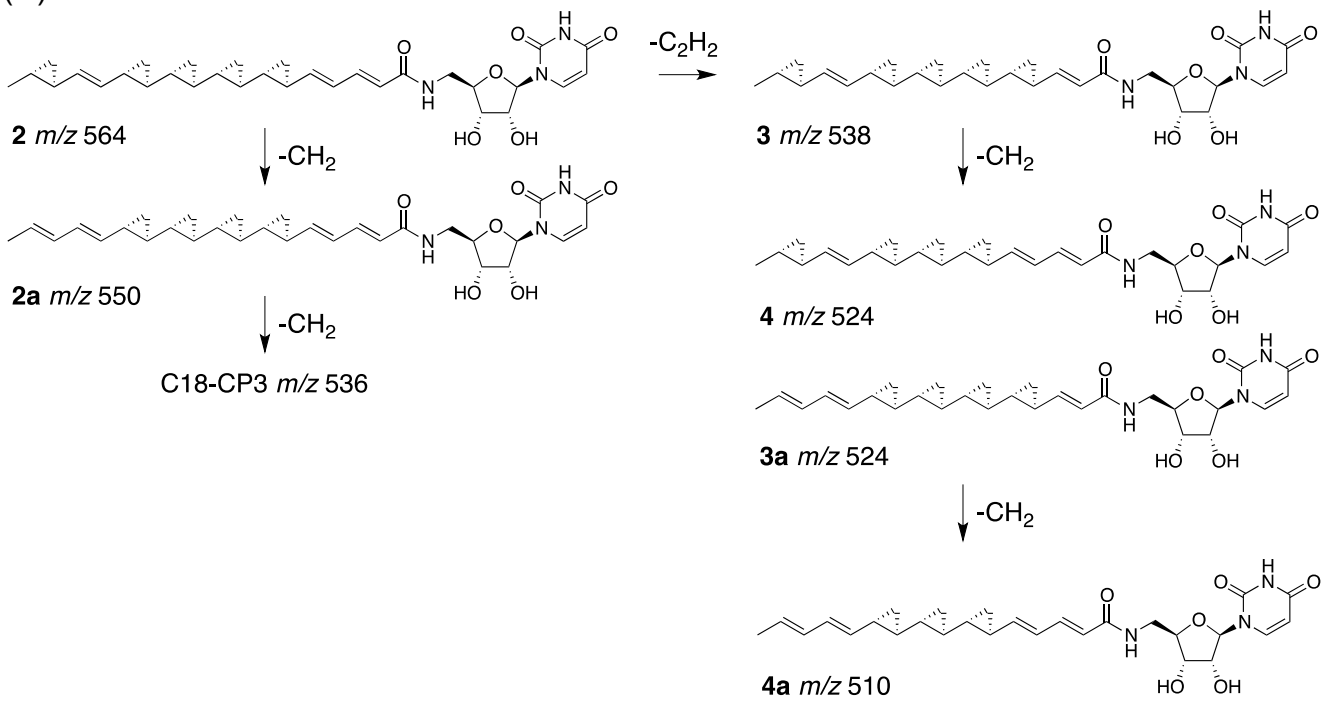

Figure S2. MS/MS spectra of **2** and **1**.

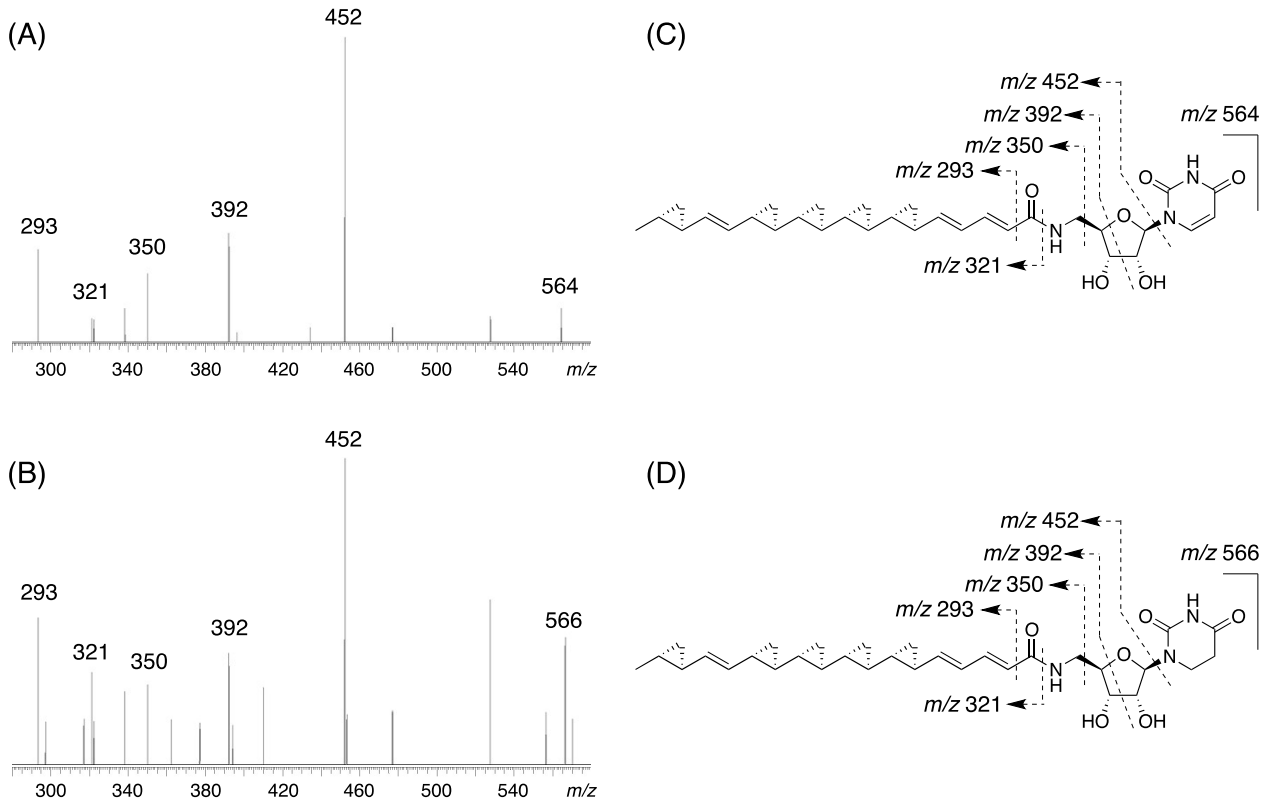

Figure S3. LC-HRMS and MS/MS analysis of (A) ^{13}C-labeled **2**, (B) ^{13}C-labeled C_{18}-CP_4 analogs, and (C) ^{13}C-labeled C_{18}-CP_3 analogs, which were obtained from the feeding experiment with L-[Me-^{13}C]methionine. In this feeding experiment shown in Figure S3-S8, a major isotopomer was found to be a fully ^{13}C-enriched sample (~50%) at a methylene carbon of the cyclopropane moiety. The carbon-13 labels are shown in the gray circles. An increased mass number of each fragmentation compared with that of non-labeled one is shown in parenthesis. (D) Summary of high resolution mass spectrometry of each compound.

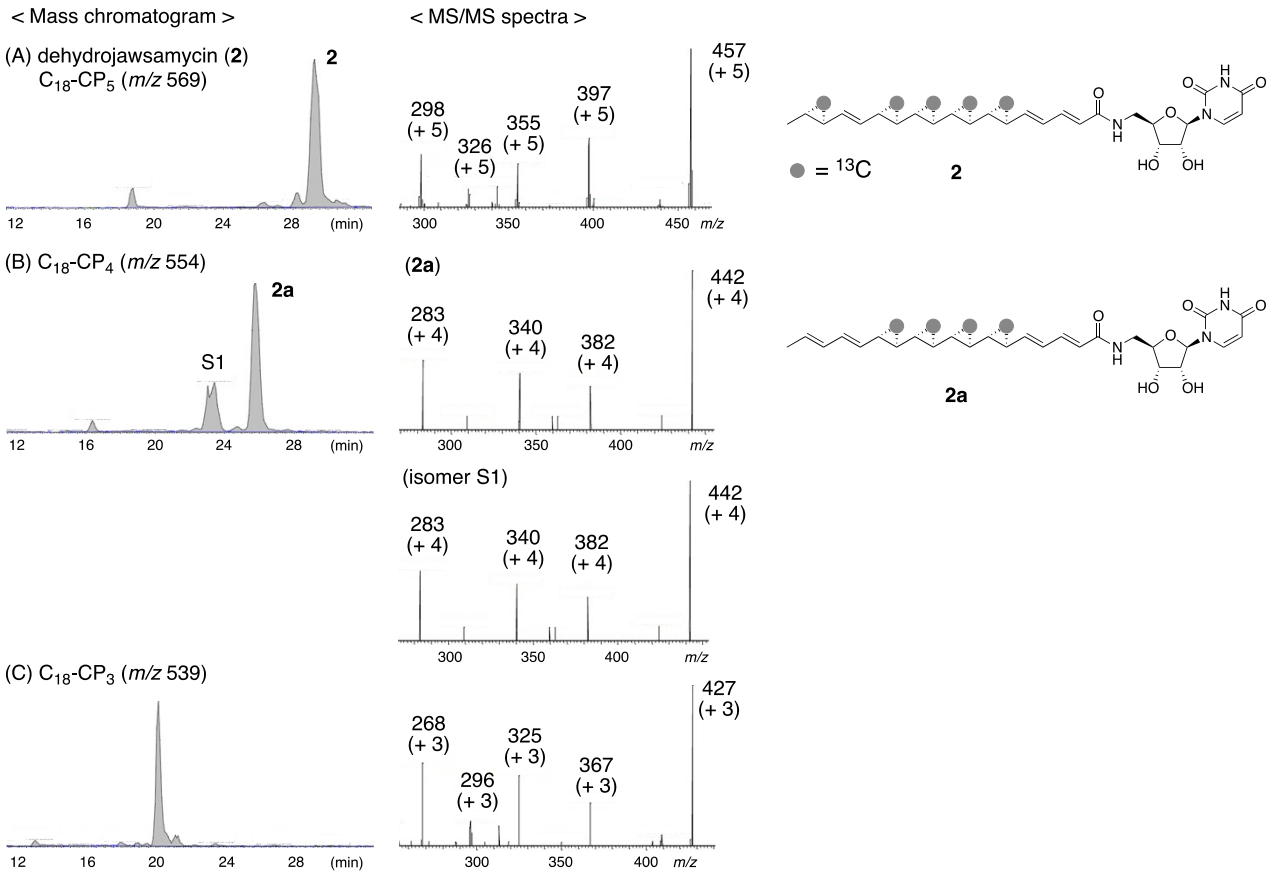

(D)

	2	2a	C_{18}-CP_4-S1	C_{18}-CP_3
calcd. for $[M+H]^+$	569.3236	554.3046	554.3046	539.2856
found	569.3232	554.3044	554.3047	539.2863

Figure S4. LC-HRMS and MS/MS analysis of (A) ^{13}C-labeled **3**, (B) ^{13}C-labeled **4** and **3a**, (C) ^{13}C-labeled C_{16}-CP_3 analogs, and (D) ^{13}C-labeled C_{16}-CP_2 analog, which were obtained from the feeding experiment with L-[Me-^{13}C]methionine. The carbon-13 labels are shown in the gray circles. An increased mass number of each fragmentation compared with that of non-labeled one is shown in parenthesis. (E) Summary of high resolution mass spectrometry of each compound.

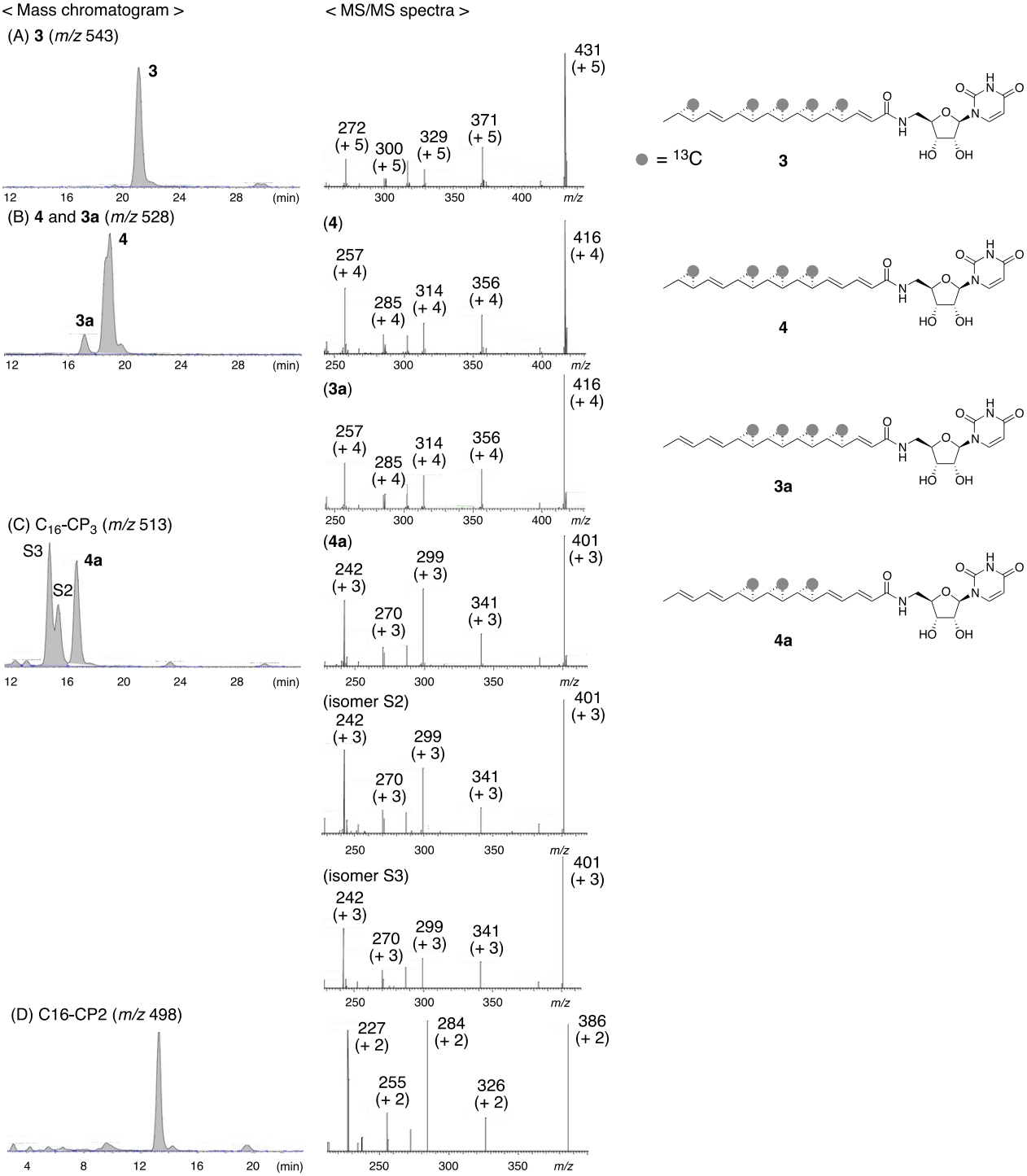

(E)

	3	3a	4	4a	C_{16}-CP_3-S2	C_{16}-CP_3-S3	C_{16}-CP_2
calcd. for $[M+H]^+$	543.3079	528.2889	528.2889	513.2699	513.2699	513.2699	498.2509
found	543.3073	528.2893	528.2889	513.2700	513.2708	513.2708	498.2509

Figure S5. LC-HRMS and MS/MS analysis of (A) ^{13}C-labeled C_{14}-CP_5 analog, (B) ^{13}C-labeled C_{14}-CP_4 analog, (C) ^{13}C-labeled C_{14}-CP_3 analogs, (D) ^{13}C-labeled C_{14}-CP_2 analogs, and (E) ^{13}C-labeled C_{14}-CP_1 analog, which are obtained from the feeding experiment with L-[Me-^{13}C]methionine. An increased mass number of each fragmentation compared with that of non-labeled one is shown in parenthesis. (F) Summary of high resolution mass spectrometry of each compound.

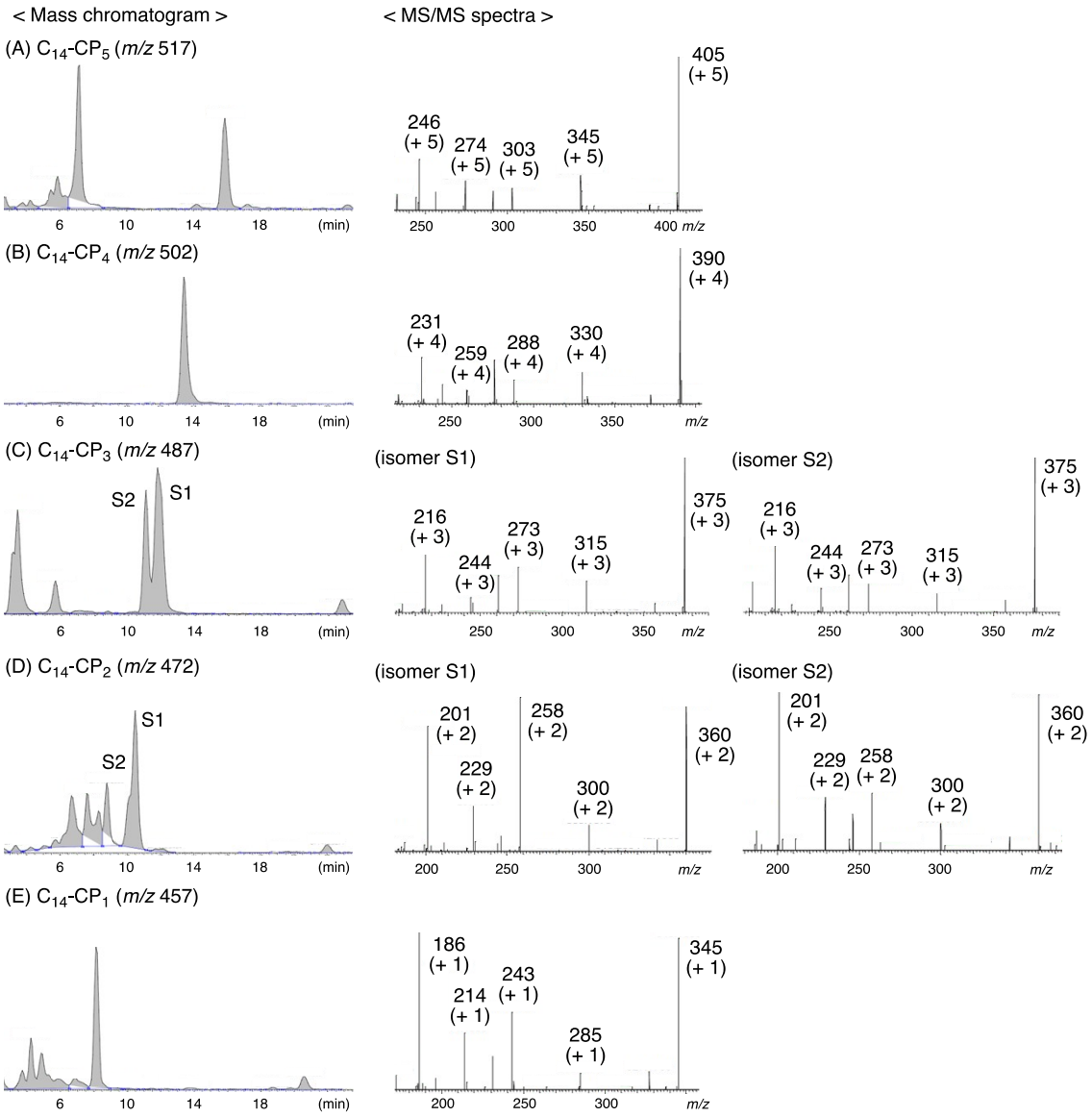

(F)

	C_{14}-CP_5	C_{14}-CP_4	C_{14}-CP_3-S1	C_{14}-CP_3-S2	C_{14}-CP_2-S1	C_{14}-CP_2-S2	C_{14}-CP_1
calcd. for $[M+H]^+$	517.2922	502.2733	487.2543	487.2543	472.2353	472.2353	457.2163
found	517.2925	502.2731	487.2545	487.2541	472.2358	472.2355	457.2165

Figure S6. LC-HRMS and MS/MS analysis of (A) ^{13}C-labeled C_{12}-CP_4 analog, (B) ^{13}C-labeled C_{12}-CP_3 analog, (C) ^{13}C-labeled C_{12}-CP_2 analog, and (D) ^{13}C-labeled C_{12}-CP_1 analogs, which are obtained from the feeding experiment with L-[Me-^{13}C]methionine. An increased mass number of each fragmentation compared with that of non-labeled one is shown in parenthesis. (E) Summary of high resolution mass spectrometry of each compound.

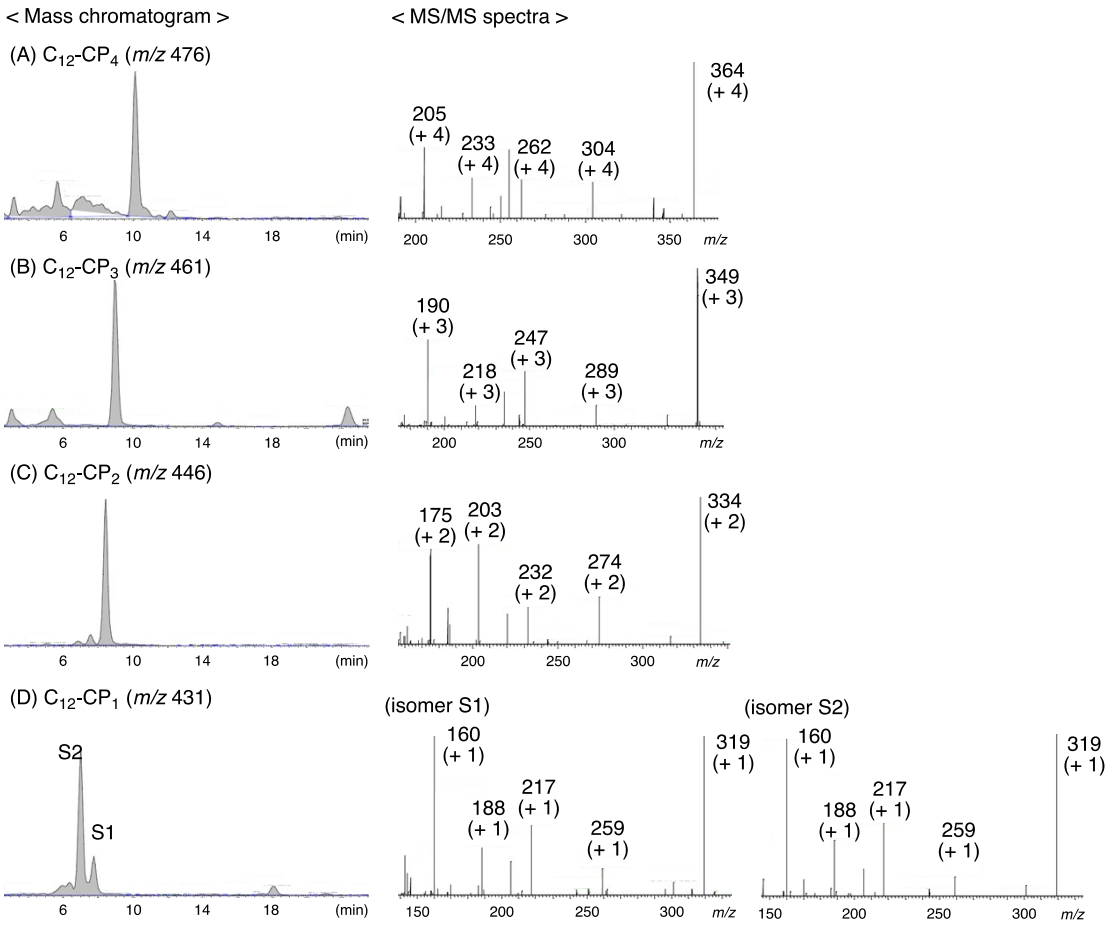

(E)

	C_{12}-CP_4	C_{12}-CP_3	C_{12}-CP_2	C_{12}-CP_1-S1	C_{12}-CP_1-S2
calcd. for $[M+H]^+$	476.2576	461.2386	446.2196	431.2006	431.2006
found	476.2578	461.2389	446.2198	431.2010	431.2013

Figure S7. LC-HRMS and MS/MS analysis of (A) ^{13}C-labeled C_{10}-CP_1 analog, which are obtained from the feeding experiment with L-[Me-^{13}C]methionine. An increased mass number of each fragmentation compared with that of non-labeled one is shown in parenthesis. (B) Summary of high resolution mass spectrometry of each compound.

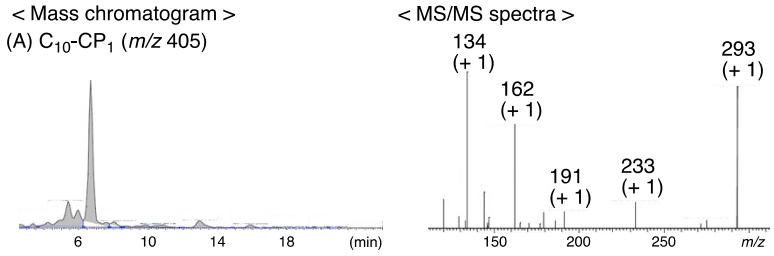

(B)

	C_{10}-CP_1
calcd. for $[M+H]^+$	405.1850
found	405.1861

Figure S8. LC-HRMS and MS/MS analysis of (A) ^{13}C-labeled C_8-CP_1 analog and (B) ^{13}C-labeled C_8-CP_0 analog, which are obtained from the feeding experiment with L-[Me-^{13}C]methionine. An increased mass number of each fragmentation compared with that of non-labeled one is shown in parenthesis. (C) Summary of high resolution mass spectrometry of each compound.

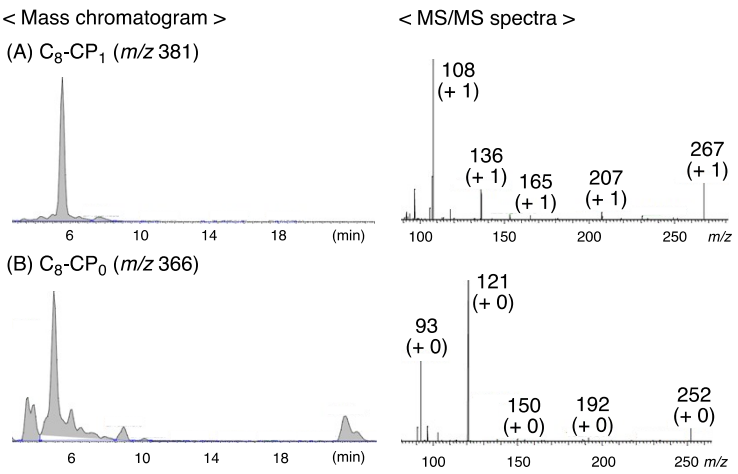

(C)

	C_8-CP_1	C_8-CP_1
calcd. for $[M+H]^+$	379.1693	364.1503
found	379.1696	364.1506

Figure S9. LC-HRMS and MS/MS analysis of (A) ^{13}C-labeled **1**, (B) ^{13}C-labeled C_{18}-CP_4 analogs, and (C) ^{13}C-labeled C_{18}-CP_3 analog, which are obtained from the feeding experiment with L-[Me-^{13}C]methionine. In this feeding experiment shown in Figure S9-S13, a major isotopomer was found to be a fully ^{13}C-enriched sample (~50%) at a methylene carbon of the cyclopropane moiety. The carbon-13 labels are shown in the gray circles. An increased mass number of each fragmentation compared with that of non-labeled one is shown in parenthesis. (D) Summary of high resolution mass spectrometry of each compound.

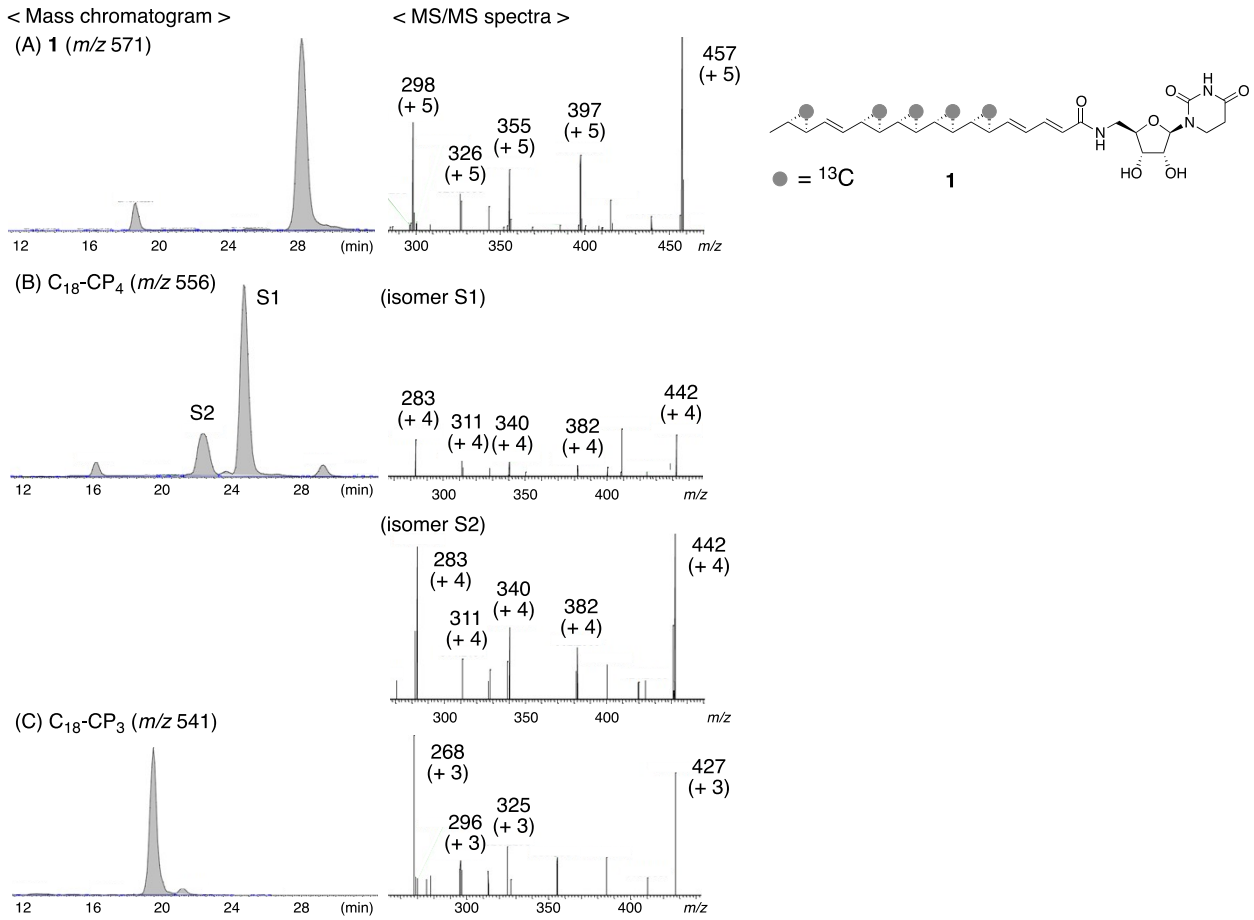

(D)

	1	C_{18}-CP_4-S1	C_{18}-CP_4-S2	C_{18}-CP_3
calcd. for $[M+H]^+$	571.3392	556.3202	556.3202	541.3012
found	571.3391	556.3196	556.3199	541.3008

Figure S10. LC-HRMS and MS/MS analysis of (A) ^{13}C-labeled C_{16}-CP_5 analog, (B) ^{13}C-labeled C_{16}-CP_4 analogs, (C) ^{13}C-labeled C_{16}-CP_3 analogs, and (D) ^{13}C-labeled C_{16}-CP_2 analog, which are obtained from the feeding experiment with L-[Me-^{13}C]methionine. An increased mass number of each fragmentation compared with that of non-labeled one is shown in parenthesis. (E) Summary of high resolution mass spectrometry of each compound.

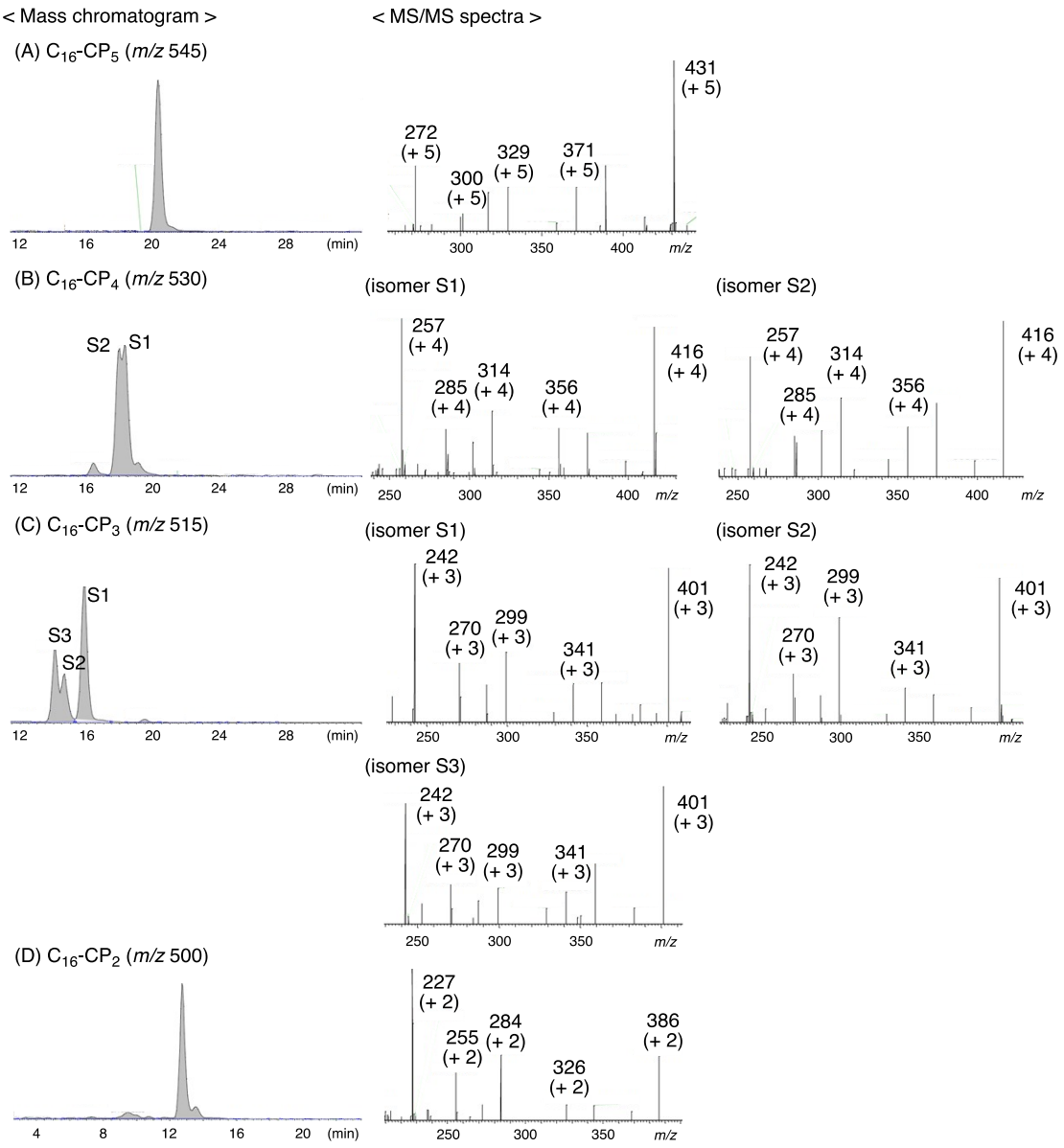

(E)

	C_{16}-CP_5	C_{16}-CP_4-S1	C_{16}-CP_4-S2	C_{16}-CP_3-S1	C_{16}-CP_3-S2	C_{16}-CP_3-S3	C_{16}-CP_2
calcd. for $[M+H]^+$	545.3236	530.3046	530.3046	515.2856	515.2856	515.2856	500.2666
found	545.3223	530.3033	530.3036	515.2848	515.2852	515.2856	500.2665

Figure S11. LC-HRMS and MS/MS analysis of (A) ^{13}C-labeled C_{14}-CP_5 analog, (B) ^{13}C-labeled C_{14}-CP_4 analog, (C) ^{13}C-labeled C_{14}-CP_3 analogs, (D) ^{13}C-labeled C_{14}-CP_2 analogs, and (E) ^{13}C-labeled C_{14}-CP_1 analog, which are obtained from the feeding experiment with L-[Me-^{13}C]methionine. An increased mass number of each fragmentation compared with that of non-labeled one is shown in parenthesis. (F) Summary of high resolution mass spectrometry of each compound.

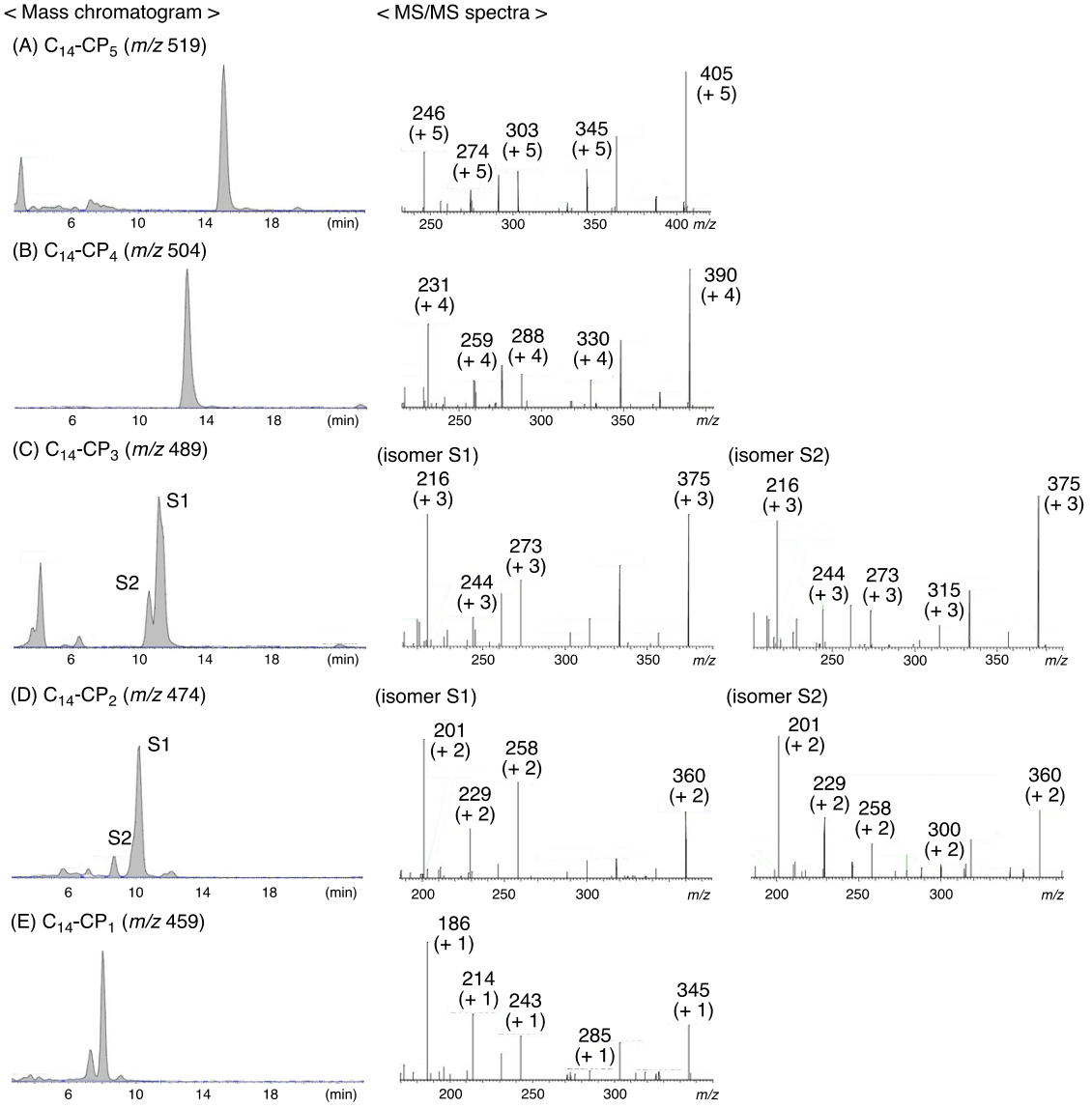

(F)

	C_{14}-CP_5	C_{14}-CP_4	C_{14}-CP_3-S1	C_{14}-CP_3-S2	C_{14}-CP_2-S1	C_{14}-CP_2-S2	C_{14}-CP_1
calcd. for $[M+H]^+$	519.3079	504.2889	489.2699	489.2699	474.2509	474.2509	459.2319
found	519.3079	504.2882	489.2694	489.2687	474.2509	474.2510	459.2320

Figure S12. LC-HRMS and MS/MS analysis of (A) ^{13}C-labeled C_{12}-CP_4 analog, (B) ^{13}C-labeled C_{12}-CP_3 analog, (C) ^{13}C-labeled C_{12}-CP_2 analog, and (D) ^{13}C-labeled C_{11}-CP_1 analogs, which are obtained from the feeding experiment with L-[Me-^{13}C]methionine. An increased mass number of each fragmentation compared with that of non-labeled one is shown in parenthesis. (E) Summary of high resolution mass spectrometry of each compound.

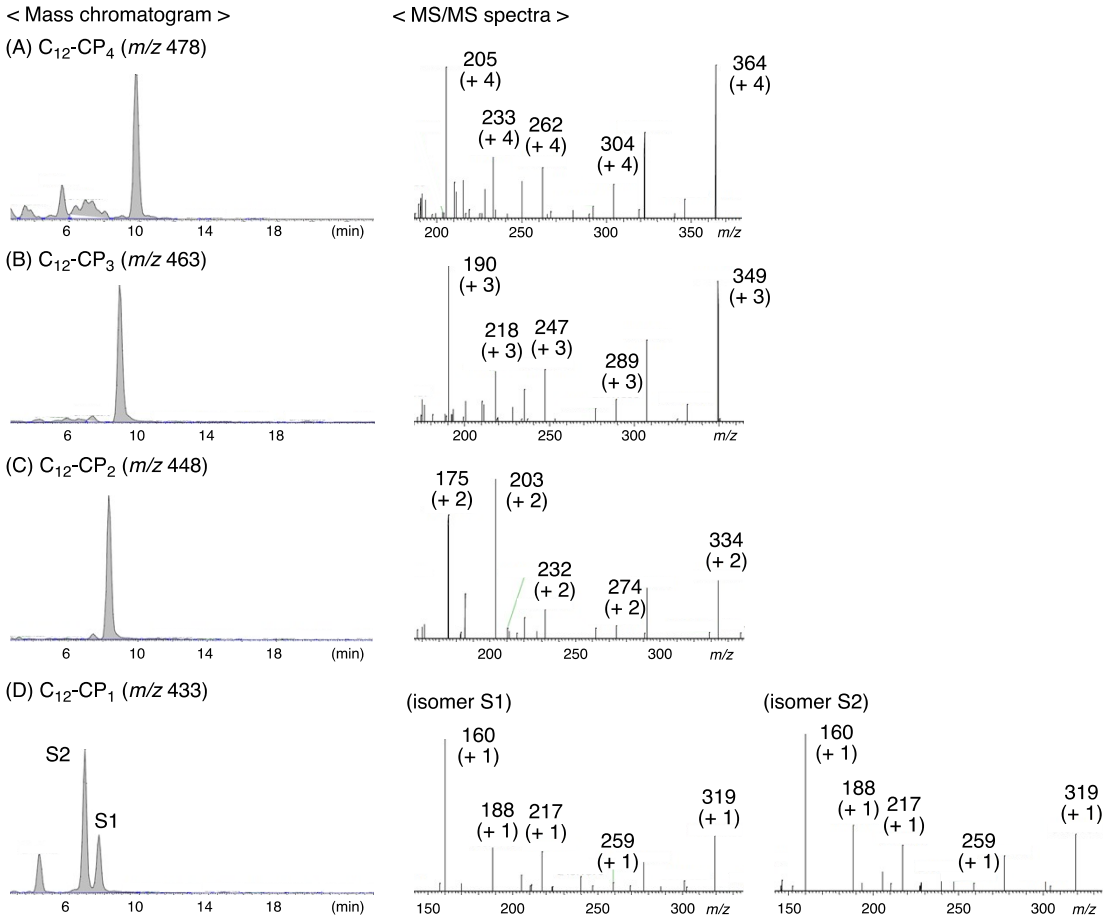

(E)

	C_{12}-CP_4	C_{12}-CP_3	C_{12}-CP_2	C_{12}-CP_1-S1	C_{12}-CP_1-S2
calcd. for $[M+H]^+$	478.2733	463.2543	448.2353	433.2163	433.2163
found	478.2740	463.2547	448.2352	433.2166	433.2165

Figure S13. LC-HRMS and MS/MS analysis of (A) ^{13}C-labeled C_8-CP_1 analog, which are obtained from the feeding experiment with L-[Me-^{13}C]methionine. An increased mass number of each fragmentation compared with that of non-labeled one is shown in parenthesis. (B) Summary of high resolution mass spectrometry of each compound.

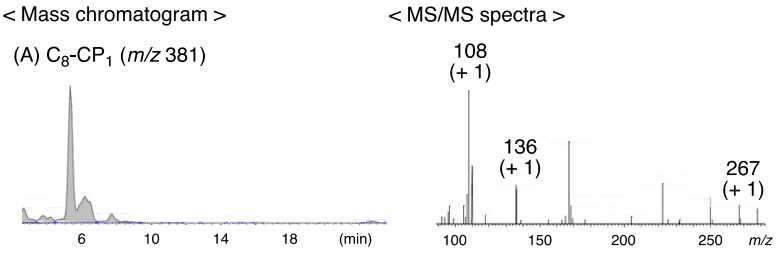

(B)

	C_8-CP_1
calcd. for $[M+H]^+$	381.1850
found	381.1861

Figure S14. MS analysis of crude metabolites from jawsamycin producing *S. fervens* HP-891.

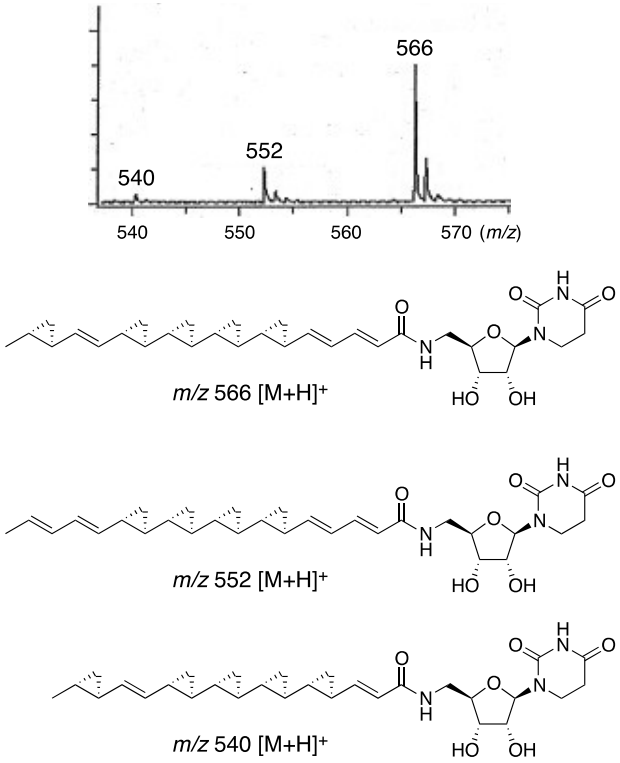

Scheme S1. Proposed biosynthetic pathway for **2a**-**4a** harboring terminal conjugated diene. The isolated analogs are labeled with asterisks. Numbering of the double bond is shown on upper part of the polyketide structure.

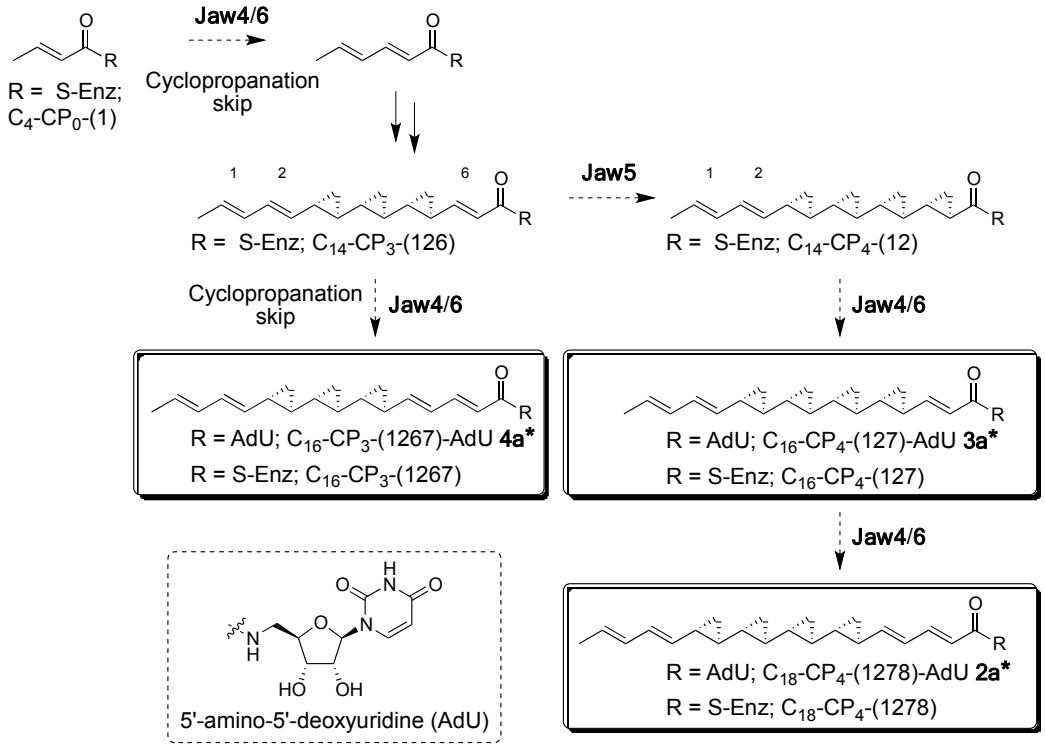

Scheme S2. Proposed biosynthetic pathway of U-106305.

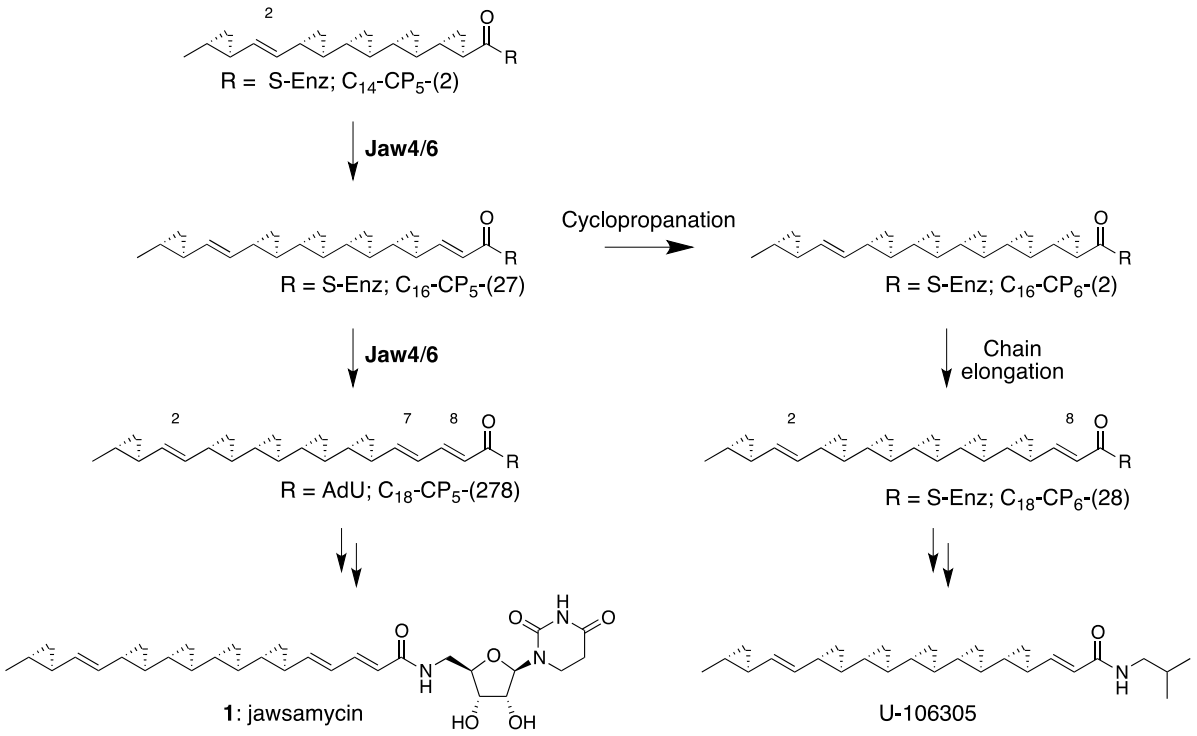

Table S1. Number of polyketide isomers of (A) **2** analogs and (B) **1** analogs. Compounds, which were not observed in the LC-HR-MS/MS analysis, are shown in horizontal bars (-). C_{10}-CP_5, C_8-CP_5, and C_8-CP_4 are not biosynthetically available and the corresponding columns are shown in grey color.

(A)

	CP_5	CP_4	CP_3	CP_2	CP_1	CP_0
C_{18}	1	2	1	-	-	-
C_{16}	1	2	3	1	-	-
C_{14}	1	1	2	2	1	-
C_{12}	-	1	1	1	2	-
C_{10}		-	-	-	1	-
C_8			-	-	1	1

(B)

	CP_5	CP_4	CP_3	CP_2	CP_1	CP_0
C_{18}	1	2	1	-	-	-
C_{16}	1	2	3	1	-	-
C_{14}	1	1	2	2	1	-
C_{12}	-	1	1	1	2	-
C_{10}		-	-	-	-	-
C_8			-	-	1	-

Table S2. Hypothetical chain elongation process. Polyketides with methyl-terminal cyclopropane are shown in red bond. Instead, those with methyl-terminal conjugated diene are shown in blue bond. Polyketide precursors of the isolated analogs are highlighted by light green color. Early stage branch point, C_4-CP_0-(1), is highlighted by yellow color. Putative side products constructed by an unexpected cyclopropanation skip are shown in square brackets but other possibilities cannot be excluded.

	CP_5	CP_4	CP_3	CP_2	CP_1	CP_0
C_{18}	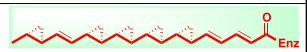 C_{18}-CP_5-(278)	[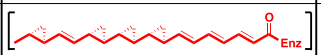] C_{18}-CP_4-(2678) 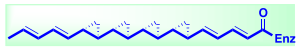 C_{18}-CP_4-(1278)	[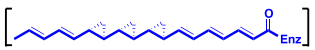] C_{18}-CP_3-(12678)			
C_{16}	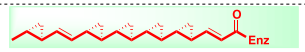 C_{16}-CP_5-(27)	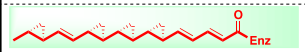 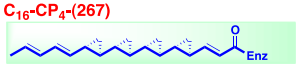 C_{16}-CP_4-(127)	[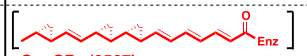] C_{16}-CP_3-(2567) 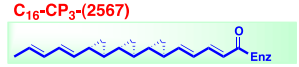 C_{16}-CP_3-(1267)	[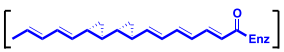] C_{16}-CP_2-(12567)		
C_{14}	 C_{14}-CP_5-(2)	 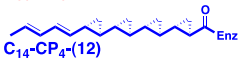 C_{14}-CP_4-(12)	[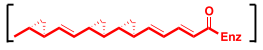] C_{14}-CP_3-(256) 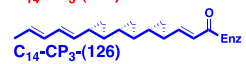 C_{14}-CP_3-(126)	[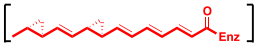] C_{14}-CP_2-(2456) 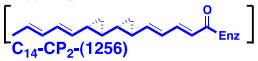 C_{14}-CP_2-(1256)	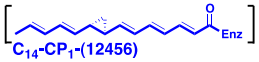 C_{14}-CP_1-(12456)	
C_{12}		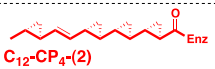 C_{12}-CP_4-(2)	 C_{12}-CP_3-(25) 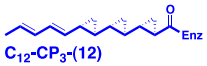 C_{12}-CP_3-(12)	[] C_{12}-CP_2-(245) 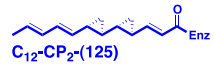 C_{12}-CP_2-(125)	[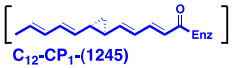] C_{12}-CP_1-(1245)	
C_{10}			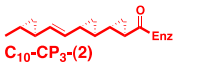 C_{10}-CP_3-(2)	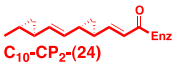 C_{10}-CP_2-(24) 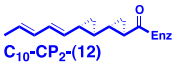 C_{10}-CP_2-(12)	[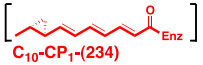] C_{10}-CP_1-(234) 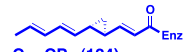 C_{10}-CP_1-(124)	
C_8				 C_8-CP_2-(2)	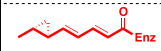 C_8-CP_1-(23) 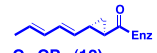 C_8-CP_1-(12)	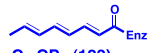 C_8-CP_0-(123)
C_6					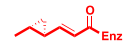 C_6-CP_1-(2)	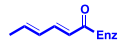 C_6-CP_0-(12)
C_4					 C_4-CP_1	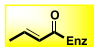 C_4-CP_0-(1)

Table S3. NMR spectral data of dehydrojawsamycin analogs.

	Dehydrojawsamycin (**2**)		C_{18}-CP_4-(1278)-AdU (**2a**)		C_{16}-CP_5-(27)-AdU (**3**)	
	δ_C	δ_H	δ_C	δ_H	δ_C	δ_H
1	165.76		165.80		165.47	
2	121.39	5.89 (d, 15.0 Hz)	121.40	5.87 (d, 15.0 Hz)	120.87	5.92 (d, 15.2 Hz)
3	139.59	6.95 (dd, 15.0, 11.2 Hz)	139.62	6.93 (dd, 15.0, 11.3 Hz)	147.21	6.13 (dd, 15.2, 9.9 Hz)
4	125.49	6.21 (dd, 15.0, 10.7 Hz)	125.50	6.10 (dd, 15.0, 11.3 Hz)	20.28	1.21-1.28 (m)
5	145.82	5.66 (dd, 10.7, 4.6 Hz)	145.89	5.63 (dd, 15.0, 9.7 Hz)	23.55	0.95-1.00 (m)
6	21.03	1.22-1.31 (m)	21.06	1.21-1.27 (m)	17.73	0.49-0.55 (m)
7	23.32	0.95-1.02 (m)	23.34	0.93-1.00 (m)	18.13	0.50-0.56 (m)
8	17.68	0.55-0.61 (m)	17.80	0.58-0.60 (m)	18.47	0.56-0.60 (m)
9	18.04	0.54-0.60 (m)	18.32	0.50-0.54 (m)	17.94	0.48-0.53 (m)
10	18.32	0.56-0.64 (m)	18.15	0.54-0.59 (m)	21.36	0.68-0.73 (m)
11	17.83	0.48-0.54 (m)	17.71	0.52-0.57 (m)	19.78	0.95-1.00 (m)
12	21.27	0.70-0.76 (m)	22.22	0.77-0.85 (m)	130.39	4.96 (dd, 5.3, 2.7 Hz)
13	19.68	0.96-1.05 (m)	20.11	1.05-1.12 (m)	130.76	4.96 (dd, 5.3, 2.7 Hz)
14	130.28	4.97 (dd, 5.1, 2.5 Hz)	135.00	5.10 (dd, 14.5, 9.0 Hz)	22.12	0.92-0.98 (m)
15	130.63	4.97 (dd, 5.1, 2.5 Hz)	127.49	5.92-6.01 (m)	14.20	0.60-0.64 (m)
16	22.02	0.95-1.02 (m)	131.54	5.88-5.95 (m)	18.41	0.98 (d, 6.0 Hz)
17	14.10	0.63-0.69 (m)	125.33	5.44-5.52 (m)	13.10	0.57-0.64 (m) 0.57-0.64 (m)
18	18.32	1.00 (d, 6.0 Hz)	17.80	1.66 (d, 6.7 Hz)	7.81	0.02-0.07 (m) 0.11 (dt, 8.4, 4.9 Hz)
19	12.99	0.52-0.64 (m) 0.52-0.64 (m)	13.01	0.51-0.61 (m) 0.51-0.61 (m)	7.81	0.02-0.08 (m) 0.02-0.08 (m)
20	7.64	0.03-0.10 (m) 0.12 (dt, 8.0, 4.9 Hz)	7.67	0.03-0.09 (m) 0.09-0.14 (m)	11.30	0.27-0.34 (m) 0.27-0.34 (m)
21	7.68	0.03-0.10 (m) 0.03-0.10 (m)	7.70	0.03-0.09 (m) 0.03-0.09 (m)	14.49	0.30-0.36 (m) 0.42 (dt, 8.4, 4.3 Hz)
22	11.19	0.30-0.37 (m) 0.30-0.37 (m)	12.04	0.38-0.46 (m) 0.38-0.46 (m)		
23	14.39	0.32-0.38 (m) 0.43 (dt, 8.2, 4.1 Hz)				
2'	150.74		151.19		150.92	
4'	163.05		163.71		163.34	
5'	101.93	5.62 (d, 8.0 Hz)	101.99	5.53 (d, 8.0 Hz)	102.05	5.59 (d, 8.0 Hz)
6'	141.30	7.67 (d, 8.0 Hz)	141.21	7.56 (br. d 6.2 Hz)	141.37	7.67 (d, 8.0 Hz)
1"	88.23	5.73 (d, 5.1 Hz)	88.40	5.68 (d, 5.2 Hz)	88.35	5.71 (d, 5.1 Hz)
2"	72.42	4.06 (t, 5.1 Hz)	72.45	4.04 (t, 5.2 Hz)	72.51	4.04 (t, 5.1 Hz)
3"	70.85	3.86 (t, 5.1 Hz)	70.88	3.84 (t, 5.2 Hz)	70.93	3.84 (t, 5.1 Hz)
4"	82.63	3.81 (dt, 6.0, 5.1 Hz)	82.58	3.78 (dt, 6.0, 5.2 Hz)	82.72	3.78 (dt, 6.4, 5.1 Hz)
5"	40.94	3.48 (dt, 13.8, 5.1 Hz) 3.27-3.35 (m)	40.97	3.45 (dt, 14.0, 5.2 Hz) 3.27-3.32 (m)	40.90	3.45 (dt, 13.9, 5.1 Hz) 3.22-3.29 (m)
2"OH		5.45 (br. s)		br		5.42 (br. s)
3"OH		5.25 (br. s)		br		5.21 (br. s)
NH		8.11 (t, 5.1 Hz)		8.14 (t, 5.2 Hz)		7.98 (t, 5.9 Hz)

Table S3. Continued.

	C_{16}-CP_4-(127)-AdU (**3a**) δ_H	C_{16}-CP_4-(267)-AdU (**4**) δ_H	C_{16}-CP_3-(1267)-AdU (**4a**) δ_H
1			
2	5.93 (d, 15.2 Hz)	5.88 (d, 15.1 Hz)	5.88 (d, 14.9 Hz)
3	6.13 (dd, 15.2, 10.0 Hz)	6.94 (dd, 15.1, 11.3 Hz)	6.95 (dd, 14.9, 11.1 Hz)
4	1.21-1.29 (m)	6.21 (dd, 15.1, 11.3 Hz)	6.21 (dd, 14.9, 11.1 Hz)
5	0.95-1.00 (m)	5.65 (dd, 15.1, 9.5 Hz)	5.65 (dd, 14.9, 9.5 Hz)
6	0.49-0.73 (m)	1.23-1.32 (m)	1.23-1.30 (m)
7	0.49-0.73 (m)	0.50-0.67 (m)	0.50-0.68 (m)
8	0.49-0.73 (m)	0.50-0.67 (m)	0.50-0.68 (m)
9	0.49-0.73 (m)	0.50-0.67 (m)	0.50-0.68 (m)
10	0.49-0.73 (m)	0.50-0.67 (m)	0.50-0.68 (m)
11	0.95-1.00 (m)	0.92-1.02 (m)	0.90-0.95 (m)
12	5.10 (dd, 14.5, 9.3 Hz)	4.97 (dd, 5.3, 2.7 Hz)	5.11 (dd, 14.6, 9.0 Hz)
13	5.94-6.03 (m)	4.97 (dd, 5.3, 2.7 Hz)	5.95-6.04 (m)
14	5.87-5.96 (m)	0.92-1.02 (m)	5.87-5.96 (m)
15	5.49 (dd, 14.5, 7.3 Hz)	0.50-0.67 (m)	5.49 (dd, 14.6, 6.9 Hz)
16	1.67 (d, 6.6 Hz)	0.99 (d, 5.9 Hz)	1.67 (d, 6.9 Hz)
17	0.57-0.64 (m)	0.50-0.71 (m)	0.50-0.68 (m)
18	0.02-0.11 (m)	0.03-0.09 (m)	0.03-0.08 (m)
19	0.02-0.11 (m)	0.30-0.46 (m)	0.41-0.48 (m)
20	0.27-0.34 (m)	0.30-0.46 (m)	
21			
22			
23			
2'			
4'			
5'	5.58 (br. s)	5.60 (d, 8.1 Hz)	5.61 (d, 8.1 Hz)
6'	7.63 (br. s)	7.66 (d, 8.1 Hz)	7.67 (d, 8.1 Hz)
1"	5.70 (d, 5.1 Hz)	5.72 (d, 5.1 Hz)	5.72 (d, 5.1 Hz)
2"	4.04 (t, 5.1 Hz)	4.04 (t, 5.1 Hz)	4.05 (t, 5.1 Hz)
3"	3.83 (t, 5.1 Hz)	3.84 (t, 5.1 Hz)	3.85 (t, 5.1 Hz)
4"	3.78 (dt, 6.0, 5.1 Hz)	3.80 (dt, 6.5, 5.1 Hz)	3.80 (dt, 6.3, 5.1 Hz)
5"	3.41-3.48 (m) 3.23-3.29 (m)	3.47 (dt, 13.6, 5.1 Hz) 3.21-3.37 (m)	3.47 (dt, 13.8, 5.1 Hz) 3.24-3.32 (m)
2"OH	5.40 (br. s)	5.42 (br. s)	5.41 (br. s)
3"OH	5.18 (br. s)	5.21 (br. s)	5.19 (br. s)
NH	7.99 (br. s)	8.11 (t, 6.0 Hz)	8.11 (t, 5.8 Hz)

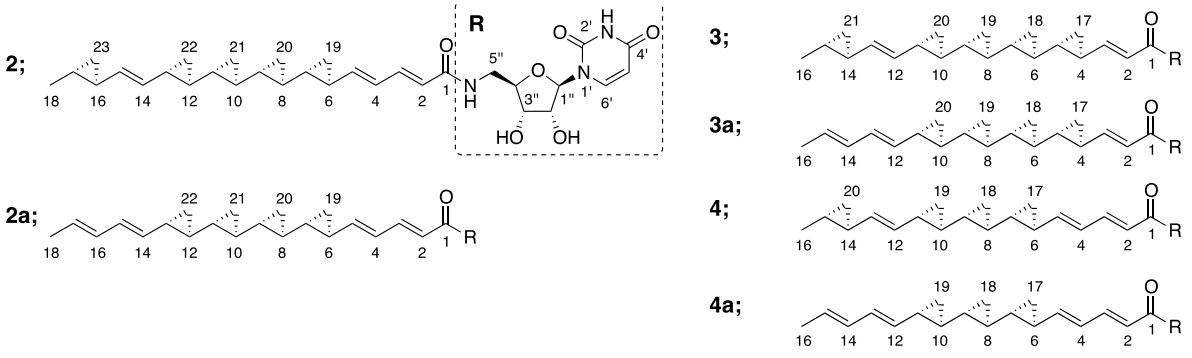

^{1}H-NMR spectrum of **2a**

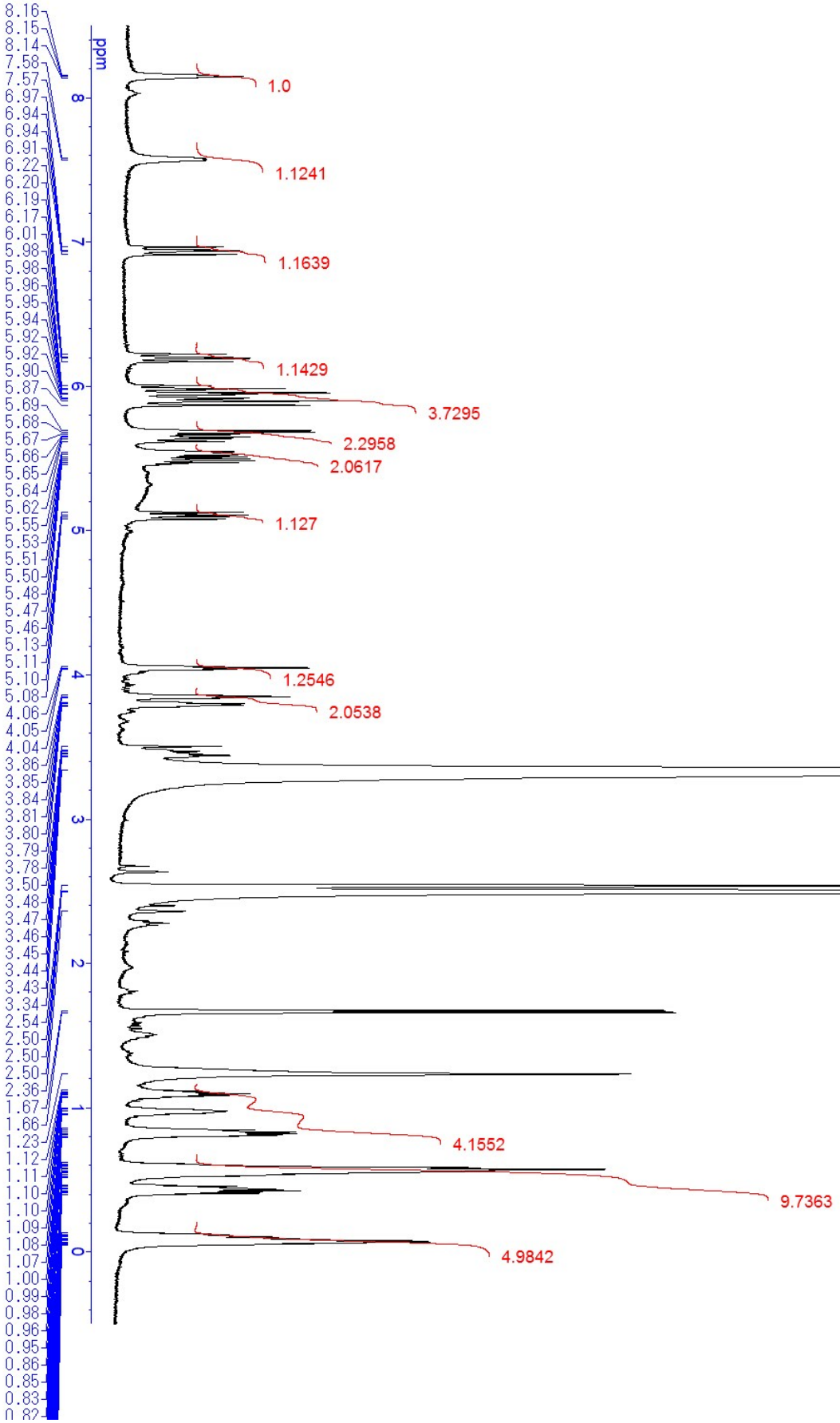

^{13}C-NMR spectrum of **2a**

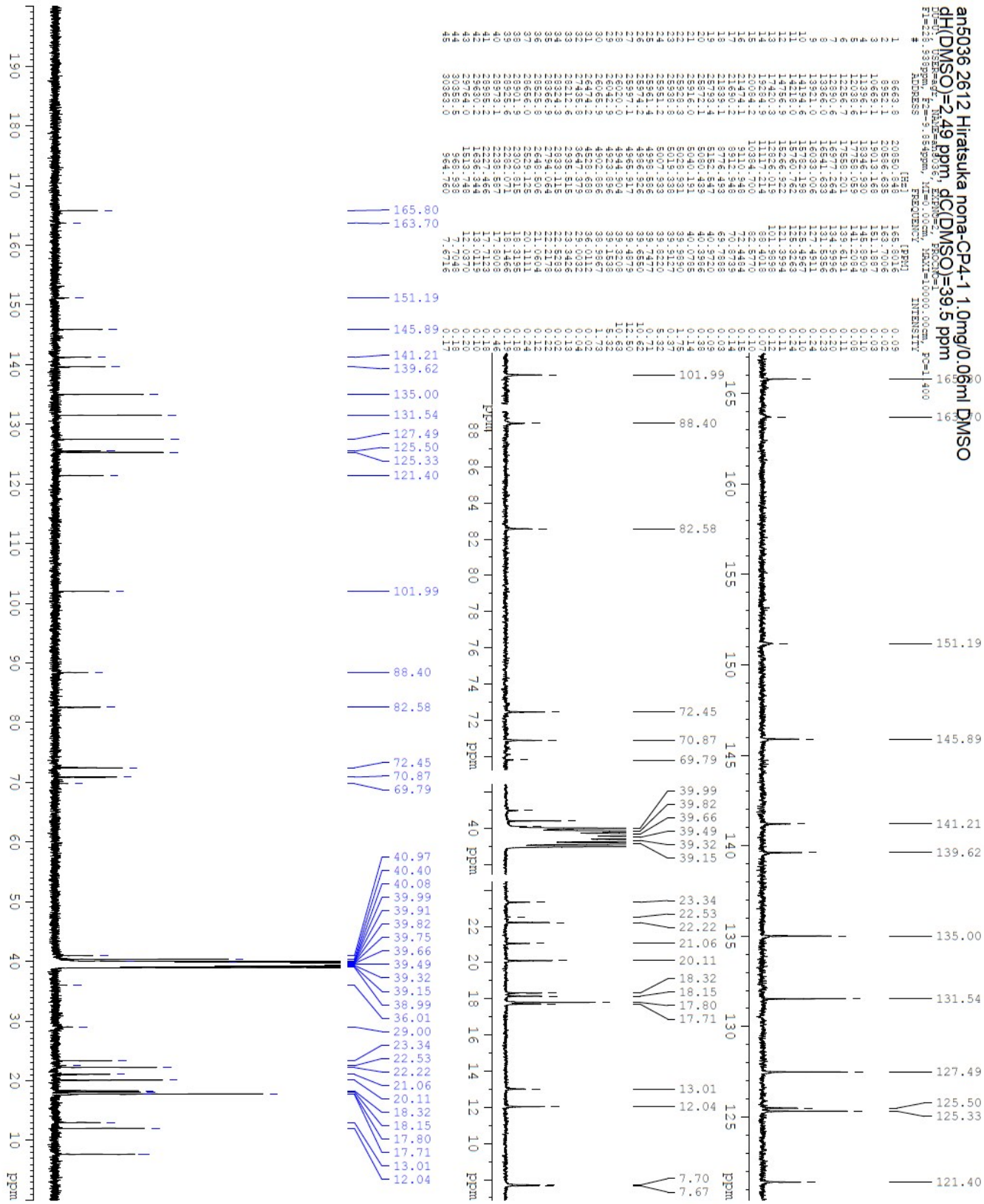

HSQC spectrum of **2a**

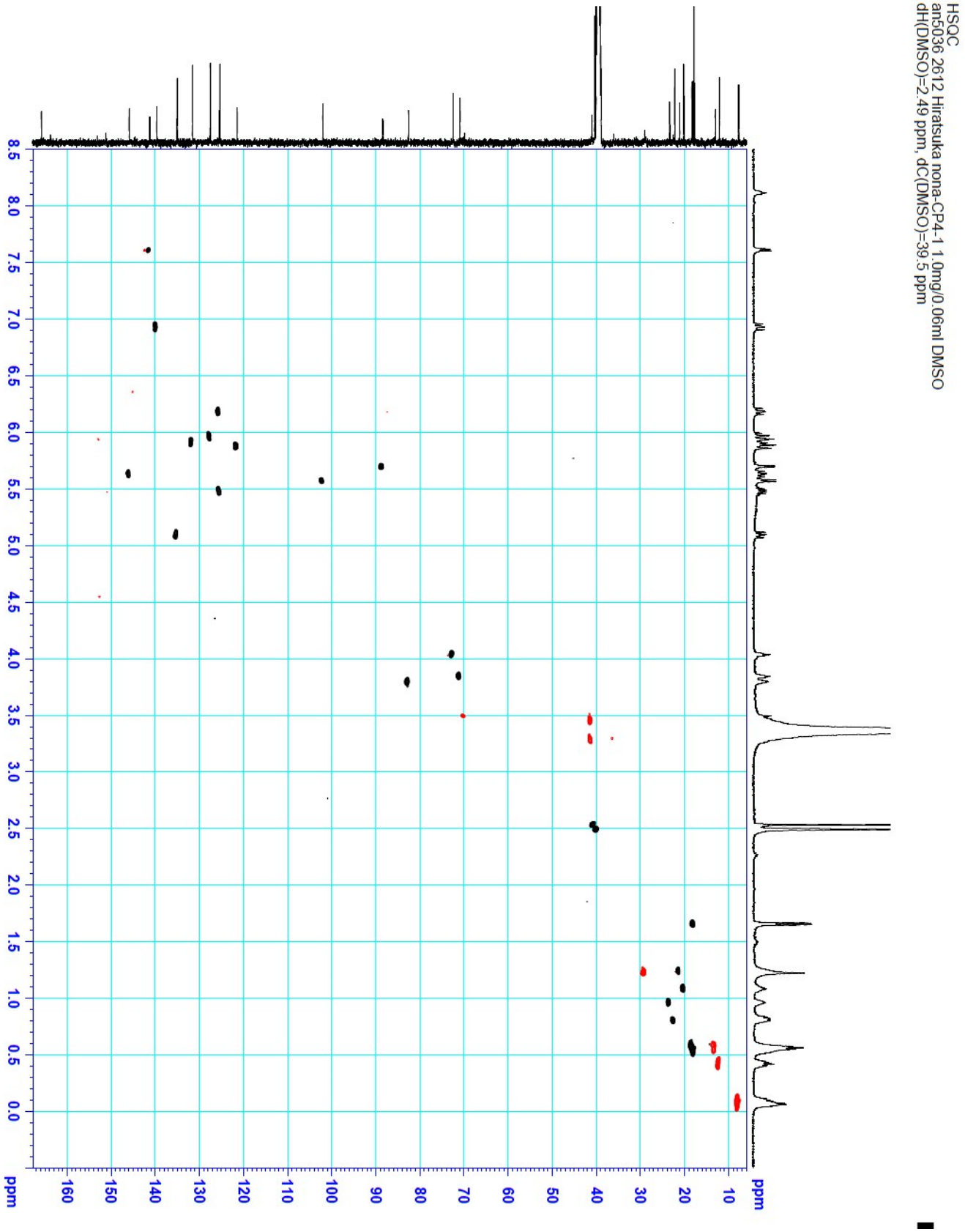

HMBC spectrum of **2a**

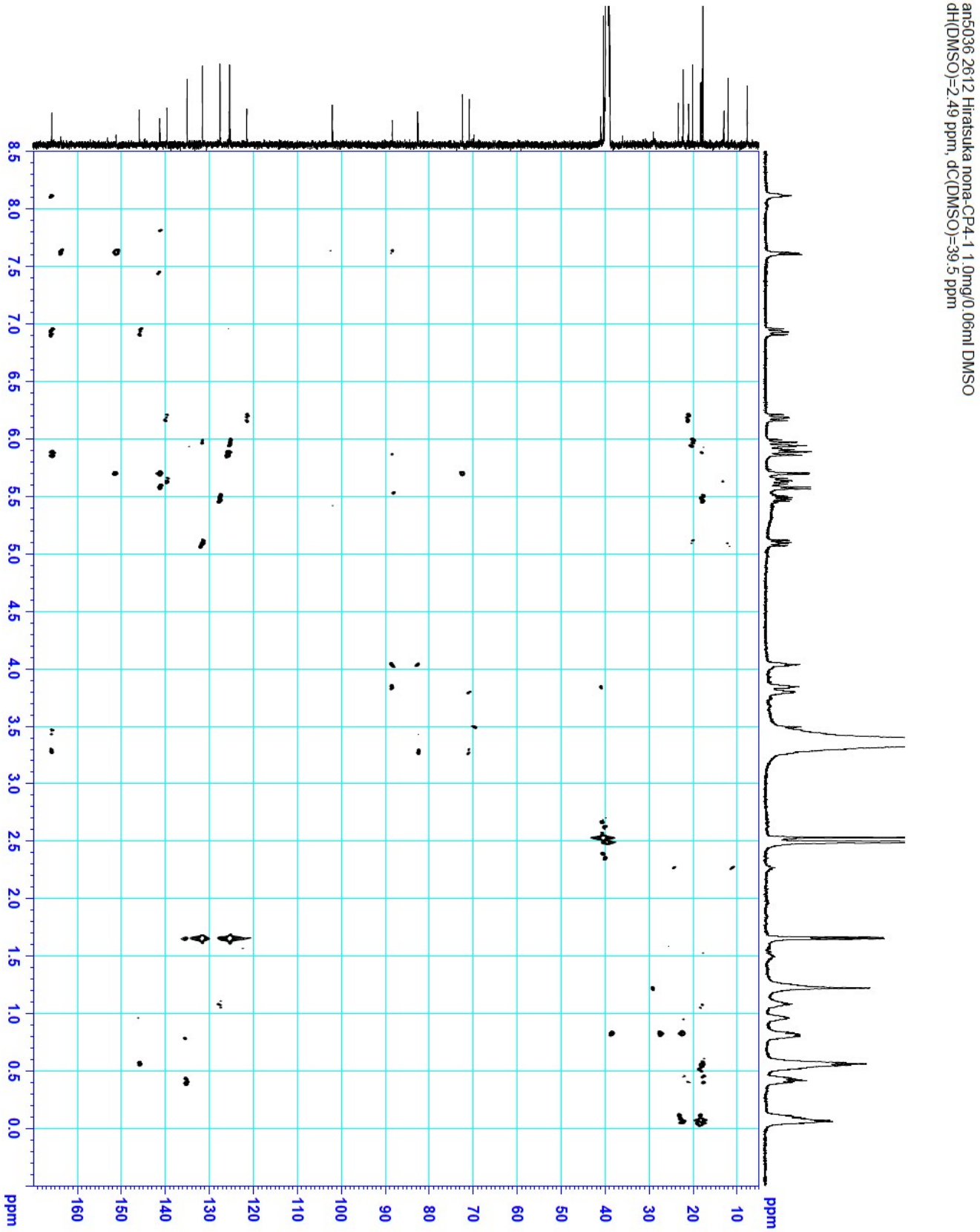

^{1}H-NMR spectrum of **3**

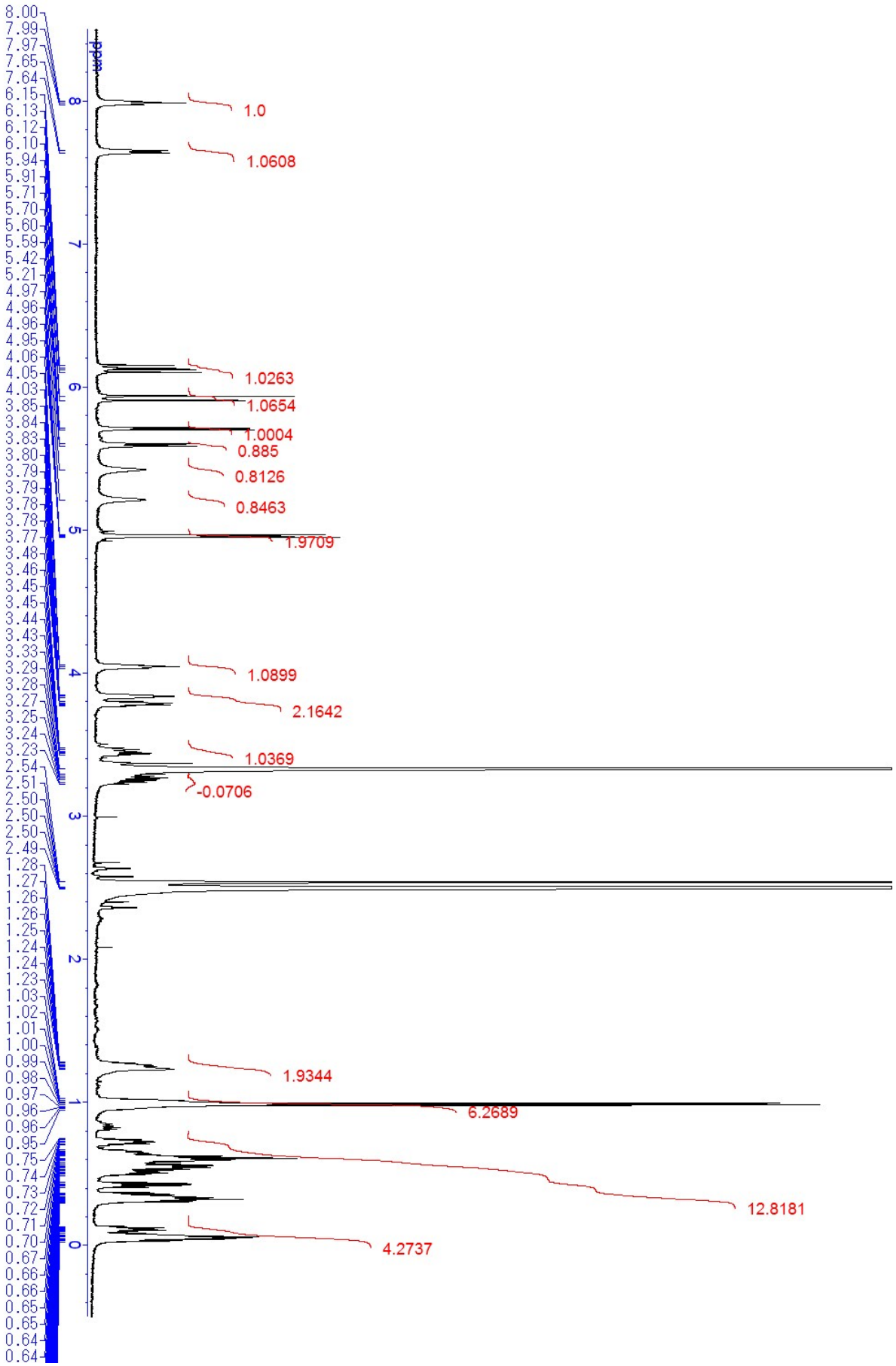

^{13}C-NMR spectrum of **3**

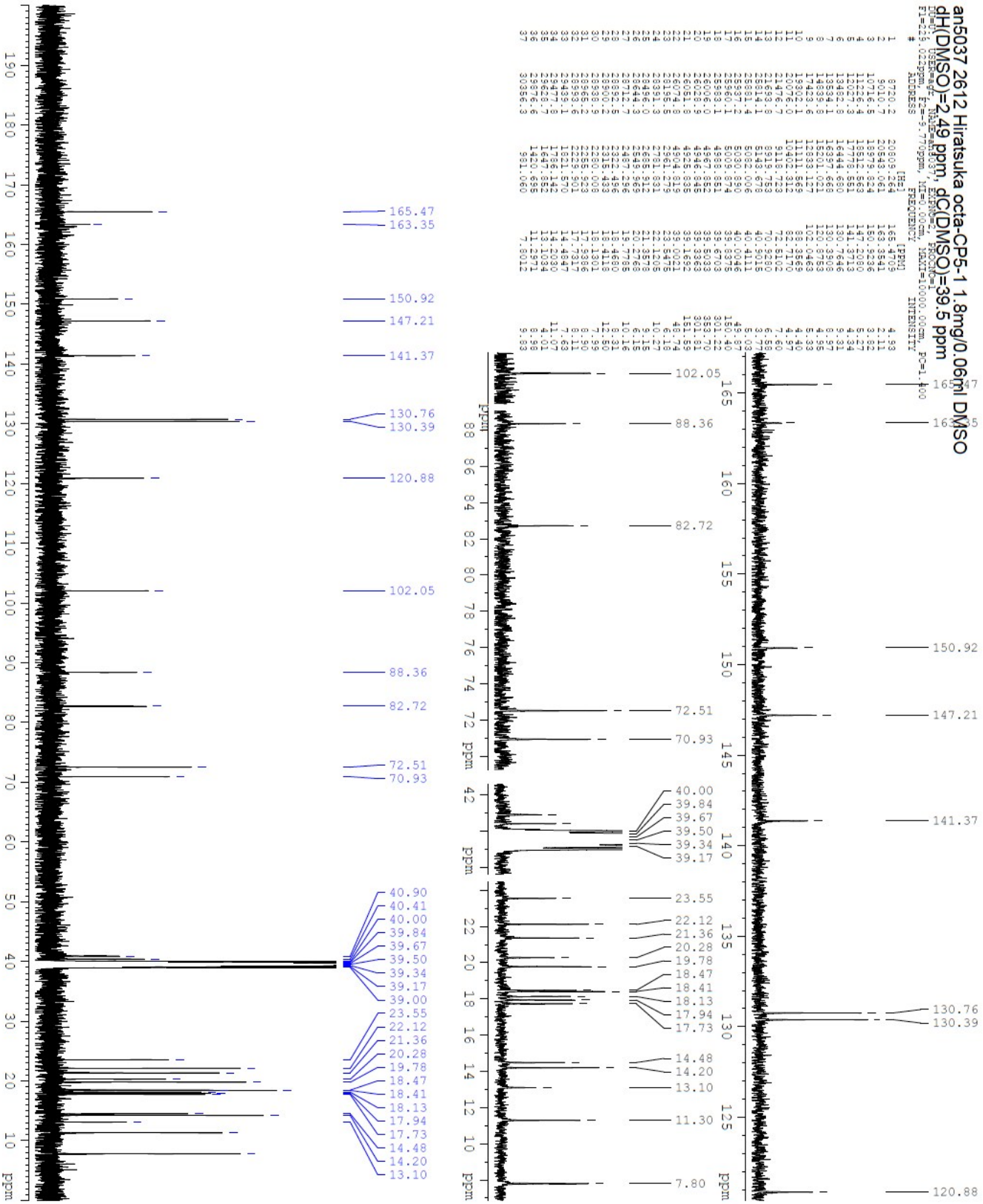

HSQC spectrum of **3**

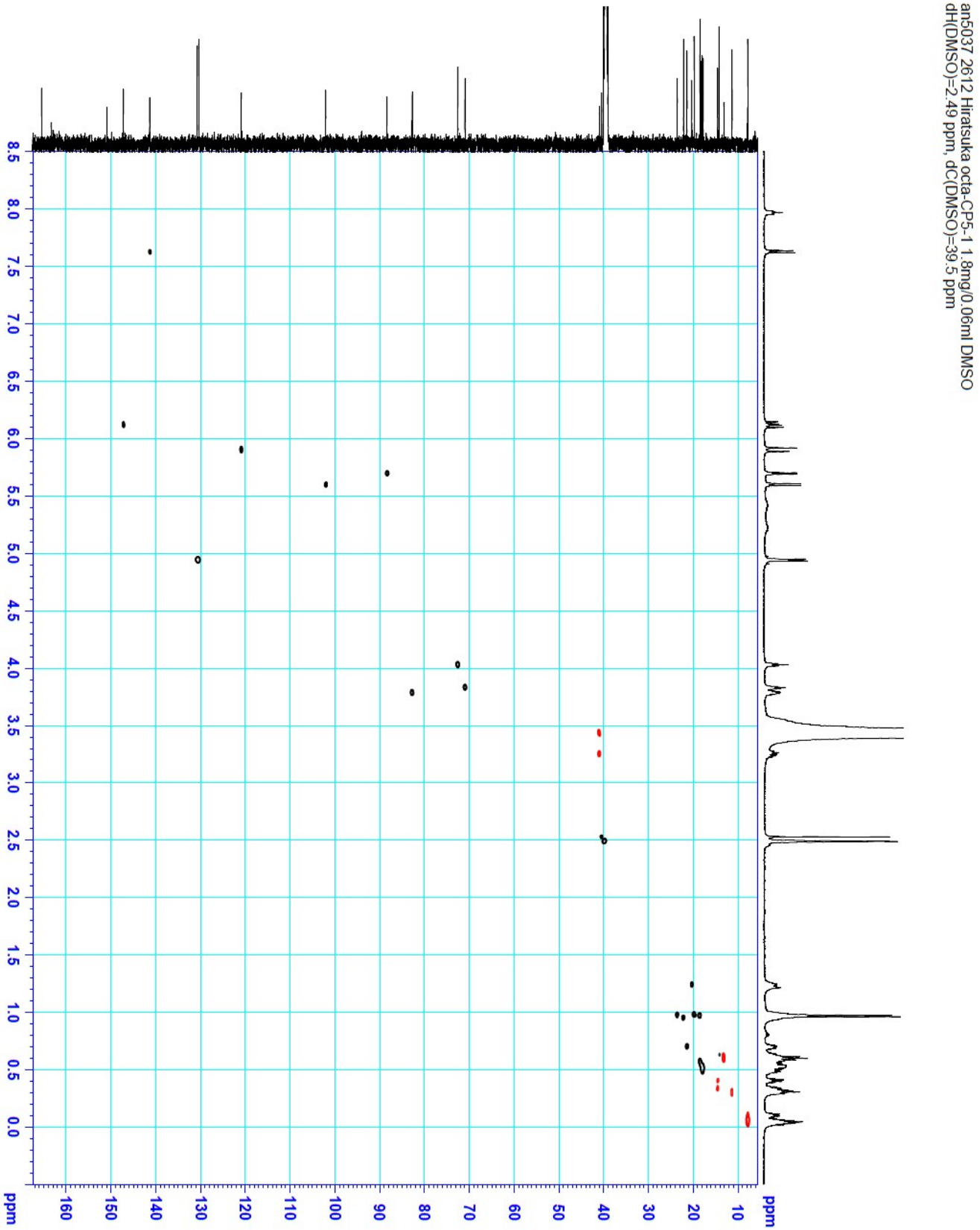

HMBC spectrum of **3**

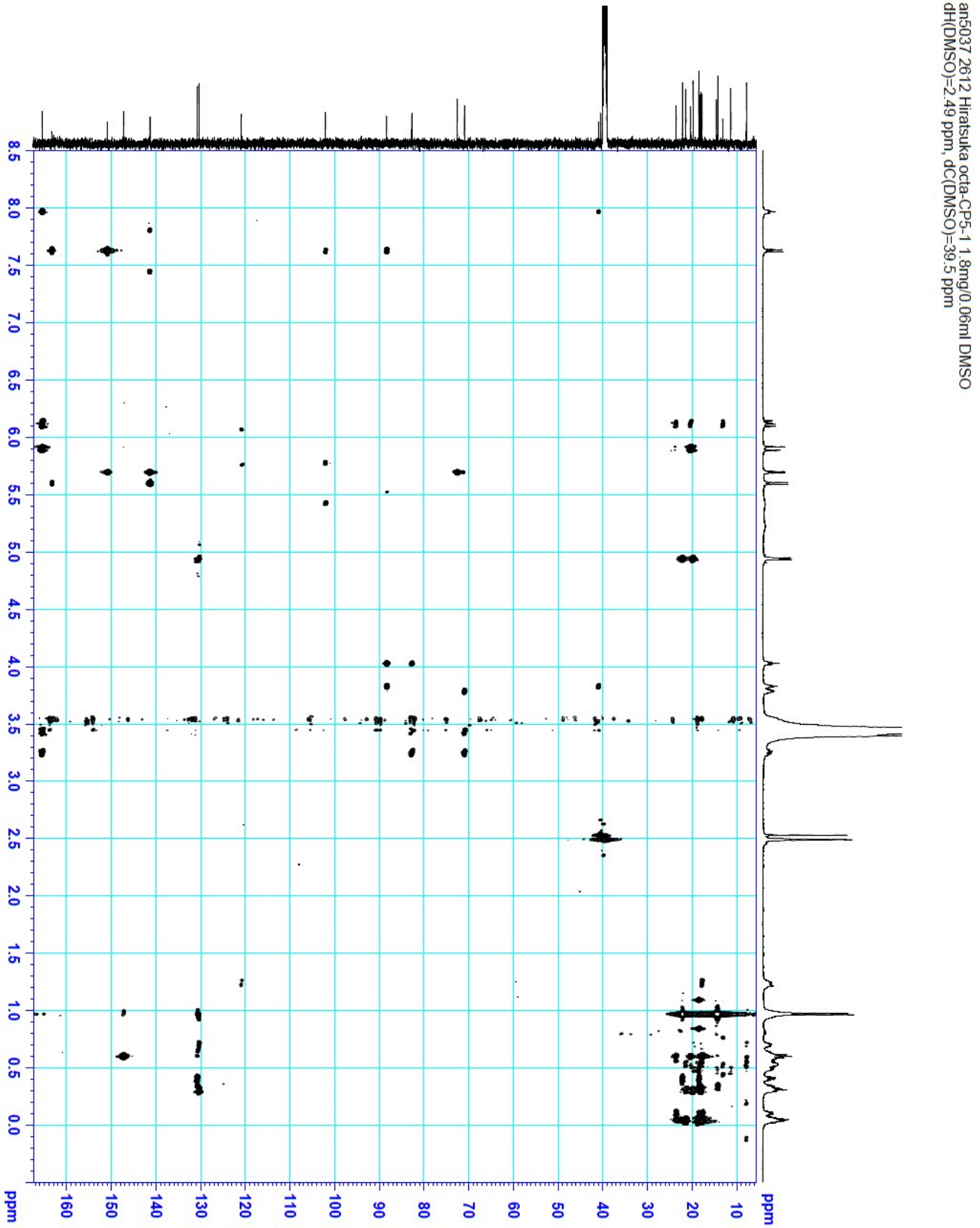

[1]H-NMR spectrum of **4**

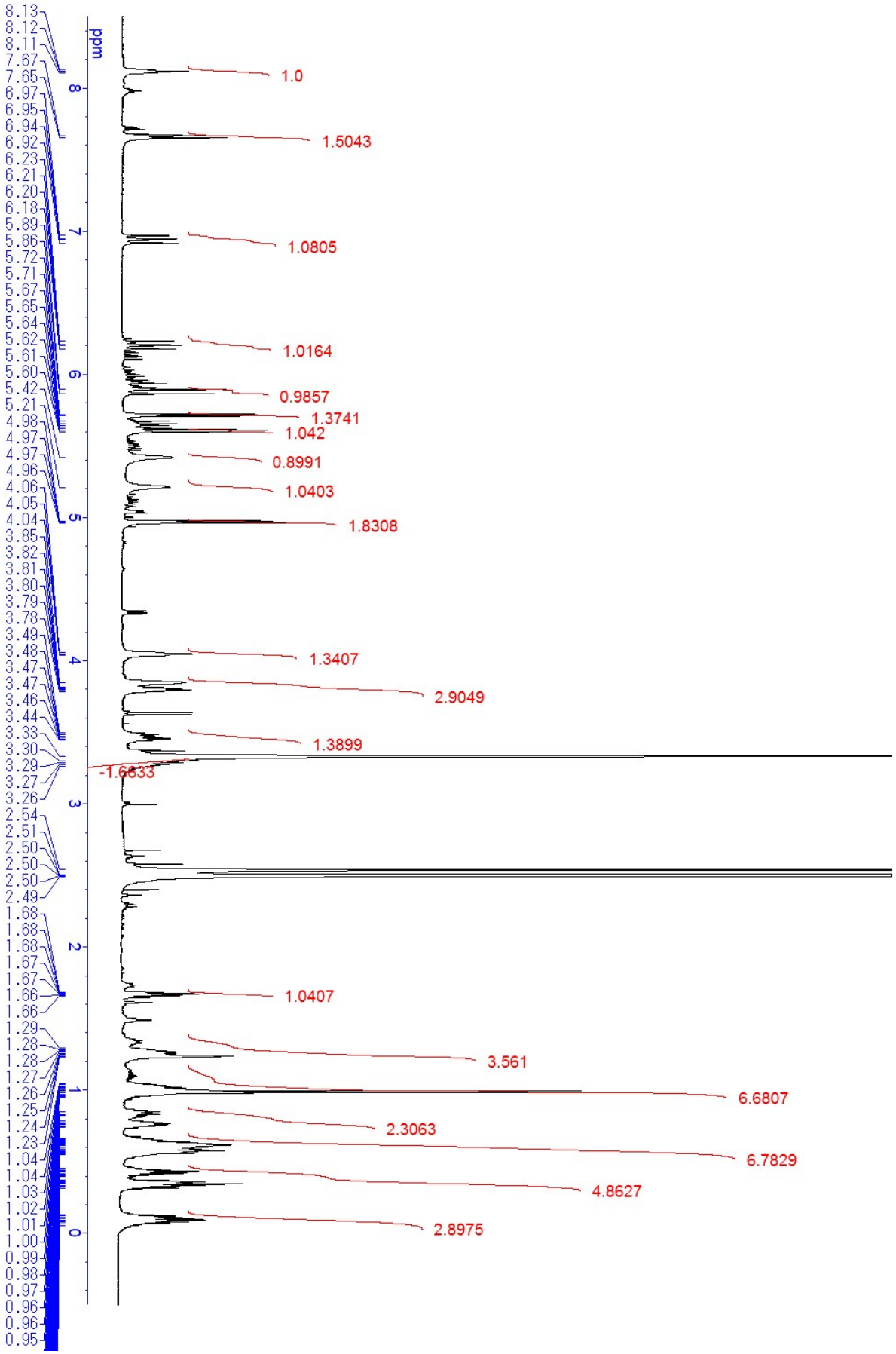

^{1}H-NMR spectrum of **3a**

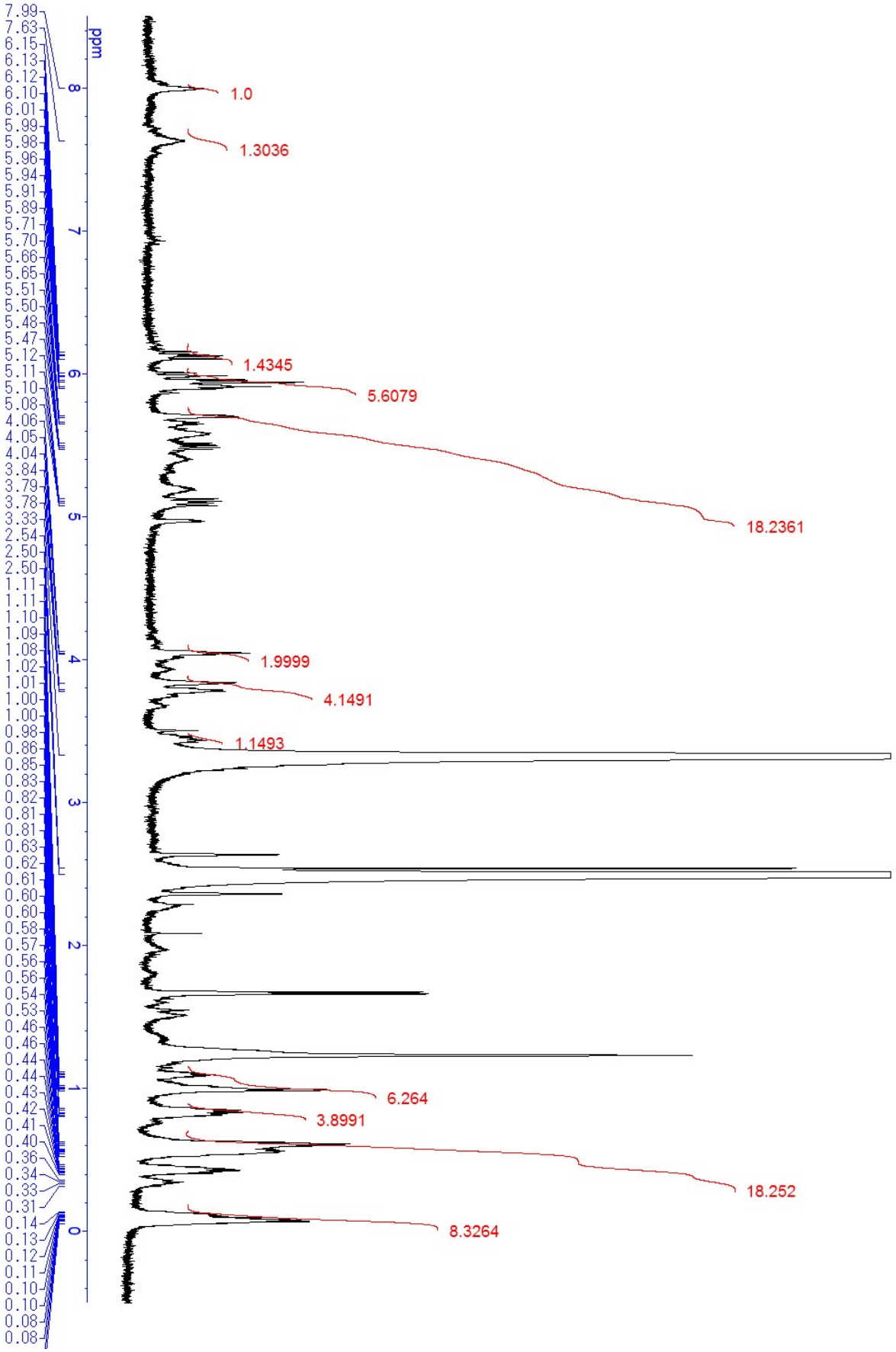

^{1}H-NMR spectrum of **4a**